Optimal Power Control, Rate Adaptation and Scheduling for UWB-based Intra-vehicular Wireless Sensor Networks

A thesis submitted in fulfilment of the requirements
for the degree of Master of Science in Engineering
Koc University, 2012

Yalcin Sadi

Graduate School of Science and Engineering
Koc University
Turkey

Koc University

Graduate School of Science and Engineering

September 2012

This is to certify that I have examined this copy of master's thesis by

Yalcin Sadi

and have found it is complete and satisfactory in all respects, and that are all revisions required by the final examining committee have been made.

Committee:

Asst. Prof. Sinem Çöleri Ergen (Advisor)

Assoc. Prof. Öznur Özkasap

Prof. Murat Tekalp

Aileme ve Bitaneme

Acknowledgements

I would like to express my sincere gratitude and profound respect to my Advisor Assist. Prof. Sinem Çöleri Ergen for her reliable guidance, inspiration, patience and valuable support. I am also grateful to members of my thesis committee Prof. Murat Tekalp and Assoc. Prof. Öznur Özkasap for their valuable comments and serving on my defense committee.

First, I thank to my family and *bitanem* Pelin for their endless faith, love and invaluable support in really hard times. Next, I would like to express my gratitudes to *en iyi dostum* Ümit, with whom I lived the best moments of a real friendship, and to Tolga for his sincere friendship which became a recourse for me for years in my problems. It is not possible to forget all shared things with my *bro's* and *leydi bro's* Burak, Bekir, Meltem, Remziye, Şebnem, Duygu, Şaziye, Nihan, Merve E., Merve G through the years. I also thank to my office friends Hüseyin, İrem, Seyhan, Nabeel who provided me a funny research environment.

Abstract

Intra-vehicular wireless sensor networks (IVWSN) is a promising new research area that can provide part cost, assembly, maintenance savings and fuel efficiency through the elimination of the wires, and enable new sensor technologies to be integrated into vehicles, which would otherwise be impossible using wired means, such as Intelligent Tire. The distinguishing properties of this network include the close interaction of the communication and control systems, strict reliability, energy efficiency and delay requirements. UWB is the most suitable technology that can meet these requirements in such a harsh environment containing a large number of reflectors operating at extreme temperatures at short distance. In this thesis, optimal power control, rate adaptation and scheduling for UWB-based IVWSN is investigated for one Electronic Control Unit (ECU) and multiple ECU cases. For one ECU case, we show that the optimal rate and power allocation is independent of the optimal scheduling algorithm. We prove the NP-hardness of the scheduling problem and formulate the optimal solution as a Mixed Integer Linear Programming (MILP) problem. We then propose a *2*-approximation algorithm, Smallest Period into Shortest Subframe First (SSF) algorithm. For the multiple ECU case where the concurrent transmission of links is possible, we formulate the optimal power control as a Geometric Programming (GP) problem and optimal scheduling problem as a MILP problem where the number of variables is exponential in the number of the links. We then propose a heuristic algorithm, Maximum Utility based Concurrency Allowance (MUCA) algorithm, based on the idea of improving the performance of the SSF Algorithm significantly in the existence of multiple ECUs by determining the sets of maximum utility.

Özetçe

Araç içi kablosuz algılayıcı ağları sağladığı parça, onarım ve bakım giderlerindeki düşüş, kabloların çıkarılması yoluyla elde edilen yakıt verimliliği ve kablolu teknolojiyle kullanılmasına imkan olmayan Akıllı Lastik gibi yeni algılayıcı teknolojilerinin uygulanmasına elverişliliği ile ümit veren yeni bir araştırma alanıdır. Haberleşme ve kontrol sistemleriyle yakın etkileşimi, yüksek güvenilirlik, enerji verimliliği ve gecikme gereklilikleri araç içi kablosuz algılayıcı ağların ayırt edici özelliklerindendir. Bu gereklilikleri, böylesine zorlu bir ortamda ve kısa mesafede karşılayabilecek en uygun iletişim teknolojisi ultra geniş bantlı iletişimdir. Bu tezde, ultra geniş bant iletişim tabanlı araç içi kablosuz algılayıcı ağları için optimum güç kontrolü, veri gönderim hızı adaptasyonu ve çizelgeleme tekniği bir ve birden fazla Elektronik Kontrol Ünitesi (EKÜ) için incelenmektedir. Bir EKÜ bulunan ağda, optimum güç kontrolünün ve veri gönderim hızı adaptasyonunun çizelgeleme algoritmasından bağımsız olduğu gösterilmiştir. Çizelgeleme problemi için optimal çözüm, polinom zamanda çözülemeyen bir Karışık Doğrusal Tamsayı Programlama problemi olarak formülleştirilmiştir. Bunun üzerine, sabiti 2 olan bir yaklaşım algoritması çizelgeleme problemi için tasarlanmıştır. Algılayıcıların eşzamanlı gönderiminin mümkün olduğu, birden fazla EKÜ bulunan ağda, optimum güç kontrolü problemi polinom zamanda çözülebilen bir Geometrik Programlama problemi olarak; optimum çizelgeleme problemi ise algılayıcı sayısına göre üstel sayıda değişkeni olan bir Karışık Doğrusal Tamsayı Programlama problemi olarak formüle edilmiştir. Bunun üzerine, çizelgeleme için, bir EKÜ bulunan ağ için tasarlanan algoritmanın birden fazla EKÜ bulunması durumunda başarımını artırma fikri üzerine kurulu buluşsal bir çizelgeleme algoritması tasarlanmıştır.

Contents

List of Figures

List of Tables

Chapter 1

Introduction

1.1 Intra-Vehicular Wireless Sensor Networks

Modern automotive technology produces vehicles with complex wired sensor networks consisting of up to 100 sensors controlled by one or multiple electronic control units (ECU) [1]. The wiring provides the connection between the sensors and the corresponding ECUs to sample and process sensor information, among ECUs to share the information with each other, and the ECUs and the battery of the vehicle to supply power. A present day wiring harness may have up to $4,000$ parts, weigh as much as 40kg and contain up to 4km of wiring. State-of-the-art manufacturing of vehicles with such amount of wiring creates design challenges increasing production, maintenance and engineering costs. Eliminating the wires can potentially reduce these costs while also offering fuel efficiency due to decreased weight and an open architecture to accommodate new sensors.

Figure 1.1 illustrates an envisioned architecture for intra-vehicular wireless sensor networks (IVWSN). The full adoption of a wireless sensor network within the vehicle may not be feasible in the near future since the experience on wireless sensor networks within the vehicle is not mature enough to provide the same performance and reliability as the wired communication that has been tested for a long time with vehicles on the road. Wireless

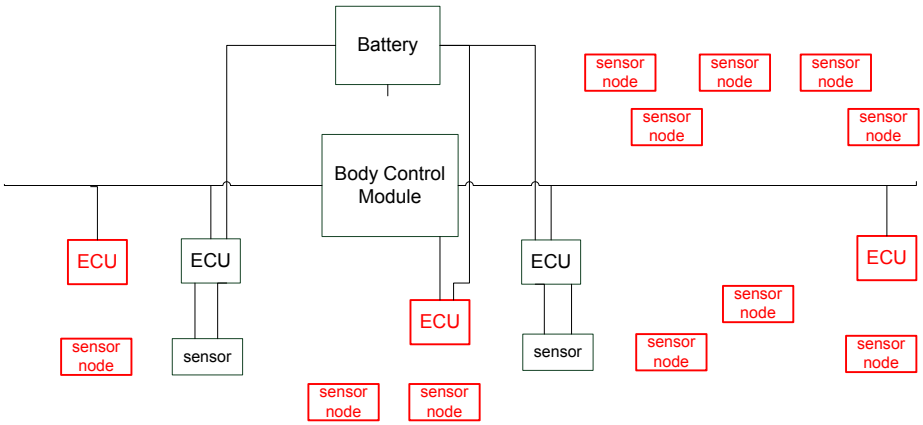

Figure 1.1: Envisioned vehicle architecture. The red colored sensor nodes and ECUs have a wireless interface. The wireless sensor nodes will connect to one of the ECUs with wireless interface.

sensor networks is expected to be deployed in the vehicle through either new sensor technologies that are not currently implemented due to technical limitations such as Intelligent Tire [2] and some sensor technologies for non-critical vehicle applications either requiring a lot of cabling such as park sensors or not functioning well enough due to cabling such as steering wheel angle sensors. Once the robustness of these wireless applications are proven within the vehicle, it will be possible to remove the cables between the existing sensors and ECUs serving more critical vehicle applications [3]. The wires between the ECUs may also be removed to replace the popular controller area network (CAN) bus in the future as an extension of this envisioned architecture however may be much harder to realize due to very high reliability requirements therefore is out of the scope of this thesis.

IVWSN is a Wireless Networked Control System (WNCS) where the sensors exchange information with the controllers using a wireless network: The data are periodically sent from the sensor nodes to the corresponding ECUs and then used in the real-time control of mechanical parts in chassis, powertrain, body and active safety domains of the vehicle [4]. Determining the *packet generation period* and *transmission delay requirement* of the

sensors given the *reliability of the underlying wireless channel*, i.e. packet success probability, to keep the system within a certain control performance has been a very active area of research in the last decade [5, 6, 7, 8, 9, 10, 11, 12]. In automotive industry, there is currently no automatic way of validating the performance of control algorithms for different packet generation period, transmission delay requirement and channel reliability values although it is under investigation. The validation would therefore be performed by extensive simulations of closed-loop models [13].

Besides satisfying the packet generation period and transmission delay requirement of the time-triggered sensors, the schedule designed for IVWSN should provide maximum adaptivity to the changes in the wireless channel characteristics and the allocation of the packets of the event-triggered sensors by distributing packet transmissions as uniformly as possible over time, and satisfy strict lifetime constraint of the IVWSN nodes since wireless communication removes the wiring harnesses for the transmission of power in addition to those for the data transmission. The schedule should be adaptive to accommodate the packet retransmission in case packets are lost due to channel fading and the packets of the nodes transmitting in an event-driven manner with minimum response time, require minimum modifications when the channel conditions of some sensor nodes change and include additional messaging to improve the performance of control algorithms. To satisfy the strict lifetime constraint of the sensor nodes on the other hand, the schedule should be predetermined and announced to the nodes so that they put their radio in sleep mode when they are not scheduled to transmit or receive a packet exploiting predetermined data generation pattern of the nodes. Moreover, the schedule should be designed jointly with the power and rate allocation of the nodes since the energy consumption during the transmission of messages is a function of the power and rate allocation of the sensor node itself together with the power and rate allocation of the sensor nodes that are scheduled to transmit concurrently [14].

1.2 Ultra Wide Band

Investigation of different modulation strategies including Radio-Frequency Identification (RFID) [15], narrowband [16, 17], spread spectrum [18] and ultra-wideband (UWB) [19, 20] in the literature demonstrated that UWB is the most suitable technology satisfying high reliability and energy efficiency requirements at short distance and low cost in such a harsh environment. UWB is often defined to be a transmission from an antenna for which the emitted signal bandwidth exceeds the lesser of 500MHz and 20% of the center frequency. This large bandwidth provides resistance to multi-path fading, power loss due to the lack of line-of-sight and intentional/ unintentional interference therefore achieves robust performance at high data rate and very low transmit power. There are two broad categories of UWB systems: impulse radio (IR) and multi-band orthogonal frequency-division multiplexing (MB-OFDM) radio. IR-UWB is more suitable for IVWSN than MB-OFDM based UWB since the energy and cost constraints of the sensor nodes cannot be met by the complex architecture of the MB-OFDM systems.

UWB communications assume the sender can adapt its transmission rate to the SINR level to meet the bit error rate (BER) requirement by changing the coding rate or modulation scheme easily [14, 21, 22, 23]. Joint optimization of transmission powers, rates and link schedule has been studied for delay constrained energy minimization in narrowband long-range wireless systems [24]. The long-range assumption however ignores the dominating circuit energy of UWB communication as mentioned before. Using the narrowband assumption on the other hand brings the maximum rate that can be sent over each link to be proportional to $log(1+SINR)$. The maximum rate achievable for UWB networks however has been demonstrated to be a linear function of $SINR$ [25, 14] and is a common assumption used in the scheduling algorithms designed for maximizing throughput in UWB networks [21, 22, 23]. The formulation of the non-convex optimization problem for rate, power and schedule in [24] is simplified by the operation of the UWB network in the linear region and inclusion of circuit energy allowing extension for the periodic data transmission of IVWSN nodes.

1.3 Related Work

The literature on scheduling algorithms is immense however none of the previously designed algorithms can be used to satisfy the packet generation period, transmission delay, energy and adaptivity requirements of IVWSN. The primary goal of the scheduling algorithms proposed for UWB networks is to maximize system throughput while providing a certain level of fairness since potential UWB applications are usually considered to be multimedia services such as voice and video conversations, video streaming and high-rate data transfer [14, 21, 22, 23]. Such a throughput maximizing objective cannot be applied to our case where the objective is to achieve the optimal value of a delay related metric, i.e. maximum adaptivity, given the transmission requirements of the nodes. The scheduling algorithms designed for delay constrained systems on the other hand mostly focus on non-periodic traffic generation patterns under two main categories: interference-free and interference-controlling scheduling. Interference-free scheduling aims to determine the optimal transmission time and duration of the packets to minimize the energy consumption of the network satisfying either a single deadline for all packets [26, 27] or individual deadlines for each packet [28, 29]. The basic assumption of decreasing the energy consumption by reducing the transmission rate in these algorithms however is not valid for short range transmissions where the circuit energy dominates the transmission energy, which is demonstrated to be true for UWB transmissions in [30]. Interference-controlling scheduling algorithms on the other hand aim to determine the best assignment of the concurrent transmissions together with their optimal power allocation [31, 32], ignoring the potential energy savings of rate adaptation. Joint optimization of transmission powers, rates and link schedule has been studied for delay constrained energy minimization only in narrowband long-range wireless systems and for non-periodic traffic generation patterns [24].

The scheduling algorithms designed for the transmission of periodic packet generating nodes have been studied for Networked Control Systems (NCS) where event-triggered controllers and actuators operate in response to spa-

tially distributed time-triggered sensor nodes. Recent communication standards for NCS such as WirelessHART [33], ISA-100.11a [34] and IEEE 802.15.4e [35] adopt a globally synchronized multi-channel Time Division Multiple Access (TDMA) with a multi-hop multi-path routing protocol. In contrast to IVWSN where the periodic data packets of sensor nodes are sent directly to the corresponding ECUs, scheduling algorithms designed for these standards mostly aim to ensure low deterministic end-to-end delay and controlled jitter to real-time traffic across a very large mesh network distributed over a large area [36, 37, 38, 39, 40]. Scheduling algorithm design for the direct transmission of the periodic data packets of the sensor nodes to their corresponding ECUs for the case where no concurrent transmissions are allowed is similar to the scheduling of multiple periodic controller tasks running on a computing platform, which mostly adopt Earliest Deadline First (EDF), Least Laxity First (LLF) and Deadline Monotonic (DM) scheduling [41]. However, these algorithms are not flexible enough to allow the resource allocation to additional nodes and packet retransmissions, and adapt to changes in the node requirements and wireless channel since the time slots are assigned to the tasks as soon as they are available. Moreover, none of these scheduling algorithms consider the joint optimization of scheduling, power and rate allocation to meet the delay, reliability, energy and adaptivity requirements of the network.

1.4 Original Contributions

The goal of this thesis is to determine the optimal power control, rate adaptation and scheduling algorithm for UWB-based IVWSNs that provides maximum level of adaptivity while meeting the packet generation period, transmission delay, reliability and energy requirements of the sensor nodes. The original contributions of this thesis are listed as follows:

- A novel scheduling problem has been formulated to provide maximum level of adaptivity while meeting the packet generation period, transmission delay, reliability and energy requirements of the sensor nodes

varying over a wide range.

- For one ECU case where no concurrent transmissions are allowed, the optimal rate and power allocation has been proved to be independent of the optimal scheduling algorithm: Maximum power and rate allocation, i.e. no power control, has been proved to be optimal. The NP-hardness of the scheduling problem has been shown and the optimal solution is formulated as a Mixed Integer Linear Programming (MILP) problem. A *2*-approximation algorithm is then proposed as a solution to this scheduling problem.

- For multiple ECU case where concurrent transmissions are allowed, it has been proved that power control is needed in contrast to previous UWB system formulations in the literature: Optimal power control is formulated as a Geometric Programming (GP) problem which is proved to be solvable in polynomial-time. Using the optimal power control, the optimal scheduling problem is formulated as a MILP problem where the number of variables is exponential in the number of the links. A heuristic algorithm is then proposed to iteratively improve the performance of the scheduling algorithm proposed for the case where no concurrent transmissions are allowed by determining the sets of maximum utility.

1.5 Organization

The rest of the thesis is organized as follows. Chapter 2 describes the system model and the assumptions used throughout the thesis. In Chapter 3, the joint optimization of power control, rate adaptation and scheduling is formulated. Chapter 4 presents the optimal power and rate allocation, the formulation of the optimal scheduling problem as a MILP problem and a 2-approximation algorithm for one ECU case where no concurrent transmissions are allowed. Chapter 5 extends the findings in Chapter 4 to the multiple ECU case where concurrent transmissions are allowed by presenting the formulation of the optimal power control as a GP problem and the

optimal scheduling problem as a MILP problem where the number of variables is exponential in the number of the links, and proposing a heuristic scheduling algorithm guaranteeing the improvement compared to one ECU case. Simulations are presented in Chapter 6. Finally concluding remarks are given in Chapter 7.

Chapter 2

System Model and Assumptions

The system model and assumptions used throughout this thesis are as follows:

1. The IVWSN contains a certain number of ECUs and a large number of sensor nodes each of which communicates to one of the ECUs as shown in Figure 1.1. ECUs do not have multi-reception capability: Any ECU can receive packet from only one sensor node at any time. Among the ECUs, one is selected as the central controller. The central controller is responsible for the synchronization of the nodes in the network and resource allocation of the active links.

2. The time is partitioned into frames. Each frame is further divided into a beacon and a number of packet slots. A guard time exists between the slots. The beacon is used by the central controller to provide time synchronization within the IVWSN and broadcast scheduling decisions for the packet slots. The scheduling decisions include the information of the time slot assignment, the data rate, transmission power and time hopping sequence corresponding to each active link. Due to the static nature of IVWSNs, the scheduling decisions are not expected to change frequently. The central controller however still continually monitors the received power and the packet success rate over each link to adjust the transmission power and rate of the nodes when needed. If

there is no need to change the scheduling decision, the beacon will only provide synchronization information. In case of such changes as failure of nodes and fluctuations of link quality, the beacon also includes the updates to the schedule. At the end of the sensor packet transmissions, an optional beacon is transmitted as needed to indicate the required packet retransmissions.

3. For time-triggered sensors, the packet generation period, transmission delay and reliability requirement, i.e. (T_l, d_l, r_l) for link l, validated for safety relevant conditions and performance specifications is given.

4. IR-UWB communications is used as the physical layer. Implementation of IR-UWB can be achieved by pulse-based time-hopping (TH) or pulse-based direct sequence (DS), or both as specified in IEEE 802.15.4a standard [42]. In the following, TH-UWB is used as an example. However, the principles can be extended to DS-UWB systems. In TH-UWB [25], the information bit is transmitted with a train of very narrow pulses. The pulse repetition time $t^{(p)}$ is divided into nc chips of duration $t^{(c)}$. A single pulse is transmitted in one chip within each pulse repetition time. Unique time-hopping sequence assigned to each link allows both smoothing the spectrum of the signal and mitigating the multi-user interference.

   In IR-UWB physical layer, the maximum achievable rate of link l is given by

$$x_l \leq K \frac{p_l h_{ll}}{\beta_l \left(N_0 + \sum_{k \neq l} p_k h_{kl} t^{(p)} \gamma \right)} \tag{2.1}$$

   where K is a system constant that maps the SNIR (Signal to Noise plus Interference Ratio) level at the receiver to the achievable transmission rate, N_0 is the background noise energy plus interference from non-UWB systems, p_l is the transmit power used on link l, h_{ll} is the attenuation of the link l, h_{kl} is the attenuation from the transmitter of link k to the receiver of link l, $t^{(p)}$ is the pulse repetition time, γ is a parameter depending on the shape of the UWB pulse and β_l is the

threshold for the ratio of SNIR to the rate of link l which is mapped from the reliability requirement, i.e. packet success probability, r_l of link l as a function of channel characteristics, modulation, channel coding, diversity and receiver design. This formulation for the maximum achievable transmission rate is based on the UWB characteristics which are adaptability of the transmission rate to the SNIR level at the receiver easily achieved by changing the processing gain via adapting the number of pulses for each symbol and/or maximum time hopping shift, or using adaptive channel coding such as rate compatible punctured convolutional (RCPC) code [22] and linear relation between transmission rate and SNIR level due to the very large bandwidth.

5. Fixed determinism is usually preferred over bounded determinism in control systems since the system with a fixed delay over all sampling periods can still be considered time invariant allowing much easier analysis of its performance [9]. We therefore assume that given (T_l, d_l) requirement provided by the application for link l, the length of the time slot t_l is the same in all periods and less than or equal to d_l as shown in Figure 2.1. The time difference between consecutive time slot allocations is fixed and equal to T_l. The automotive sensor then records the data samples every T_l time unit immediately before its time slot allocation and sends one data packet consisting of these data samples.

6. For event-triggered sensors, the packets are transmitted either in the unallocated parts of the schedule as they arrive or assigned periodic time slots with T_l, d_l and r_l values chosen such that $k(T_l + d_l)$ is less than the maximum response time requirement guaranteeing the arrival of packets within maximum response time with confidence $1-(1-r_l)^k$ for high criticality applications.

7. Data priorities of the sensor nodes are determined considering their packet generation periods in such a way that the smaller the packet generation period of a sensor, the higher the priority of that sensor.

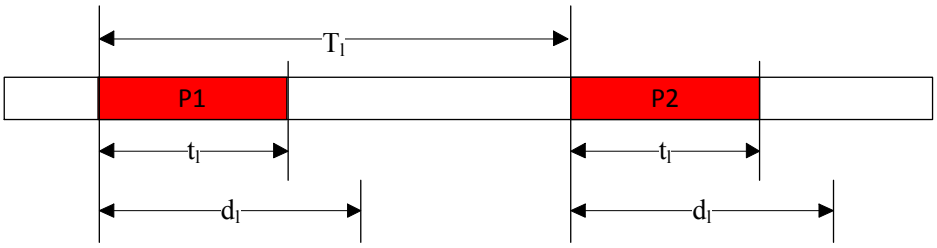

Figure 2.1: Time slot allocation of a sensor node transmitting over link l.

Data priorities of the sensor nodes with the same packet generation period is assumed to be given.

8. Packet generation period of every sensor is either a multiple or aliquot of the other packet generation periods. This assumption can be given as a constraint to the control applications.

9. We consider only the energy consumption in the transmission of the packets since they are much larger than the energy consumption in sleep mode and transient mode, which is when the node is switching from sleep mode to active mode to transmit a packet [43].

Chapter 3

Description of the Optimization Problem

The goal of the joint power control, rate adaptation and scheduling problem is to provide maximum level of adaptivity while satisfying packet generation period, transmission delay, reliability and energy requirements of the sensor nodes.

Before quantifying the adaptivity metric in the objective of the optimization problem, we illustrate the characteristics of an adaptive schedule through an example. Let us assume that we have 2 sensors of time slot lengths $t_1 = 0.1ms$ and $t_2 = 0.2ms$ and packet generation periods $T_1 = T_2 = 1ms$, and 2 sensors of time slot lengths $t_3 = t_4 = 0.3ms$ and packet generation periods $T_3 = T_4 = 2ms$. Also assume that the transmission delay requirement of these sensors is equal to their packet generation period. Then, each time interval of length $1ms$ needs to include both sensors 1 and 2 however the allocation of sensors 3 and 4 may change. The schedule given in Figure 3.1 (a) is generated by using Earliest Deadline First (EDF) scheduling policy assuming all packets are generated at the beginning of the scheduling frame of duration $2ms$ and the deadline of the packets is equal to their transmission delay requirement. EDF has been shown to be optimal for deadline constrained scheduling under various modeling assumptions [41]. Another feasible schedule that distributes the allocation of time slots uniformly over

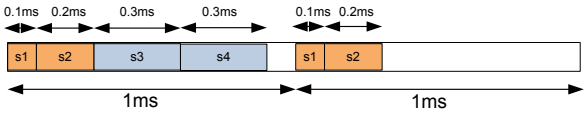

(a)

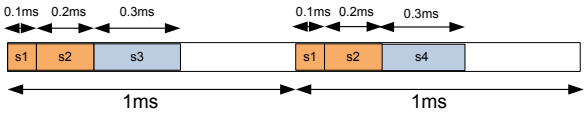

(b)

Figure 3.1: Illustration of the adaptivity requirement. a) EDF scheduling. b) Alternative schedule that distributes the allocation of time slots uniformly over time.

time is illustrated in Figure 3.1 (b). We now compare the performance of these two schedules in terms of adaptivity.

- Suppose that the transmission rate of sensor 3 needs to decrease such that the time slot length is doubled as $t_3 = 0.6ms$. The allocation in Figure 3.1 (b) is able to accommodate the new change whereas the one in Figure 3.1 (a) cannot. The allocation in Figure 3.1 (b) can also allocate additional messaging for sensor 3 with time slot length $t_3 = 0.3ms$ whereas the one in Figure 3.1 (a) cannot.

- Suppose that the transmission of the data packet of sensor 2 in the first 1ms failed. The schedule in Figure 3.1(b) includes enough space to allocate the retransmission of sensor 2 whereas the schedule in Figure 3.1(a) does not.

- Suppose that in addition to the periodic data packet generation of the scheduled sensor nodes, an additional packet of $0.3ms$ time slot length

is generated by an event-triggered sensor node at the beginning of the scheduling frame. Then in the schedule of Figure 3.1(a), the time slot of the event-triggered packet can be allocated with a delay of $1.3ms$ whereas in the schedule of Figure 3.1(b), the time slot can be allocated with a delay of $0.6ms$.

An adaptive schedule should therefore distribute node transmissions as uniformly as possible over time.

Determining the best uniform distribution of transmissions first requires determining the subframe length over which the transmissions are distributed as uniformly as possible. Let us order the nodes in increasing packet generation period such that $T_1 \leq T_2 \leq ... \leq T_L$ for L active links. We choose the subframe length S for uniform distribution objective as the minimum packet generation period T_1; i.e. $S = T_1$: The time slot for the sensor node with packet generation period T_i needs to be allocated once every T_i/S subframes, where T_i/S is an integer due to the assumption given in Chapter 2 that T_i is an integer multiple of S. For example, in Figure 3.1, subframe length $S = 1ms$. If we had chosen a smaller subframe length than $S = T_1$, say $S = T_1/2$, this may have resulted in a more uniform distribution than choosing $S = T_1$ still satisfying the periodic data generation and transmission delay requirements of the sensors. However, since a transmission cannot be done partially in different time intervals, i.e. pre-emption is not allowed, the shorter unallocated time duration at the end of the subframes may not allow changing the transmission time of the packets or allocating additional messages and retransmissions violating the adaptivity requirement. The shorter subframe length may even avoid generating feasible schedules if the length of the time slots is too large to fit in one subframe. Choosing the subframe length larger than $S = T_1$ on the other hand does not bring any advantage and result in less uniform distribution. Let us define the total active length of the subframe l, a_l, as the sum of the length of the time slots allocated in subframe l. *The objective of determining the schedule providing maximum level of adaptivity so the best uniform distribution of transmissions can therefore be quantified as minimizing the maximum total active length of all subframes,*

where the subframe length is the minimum packet generation period among the sensor nodes.

The constraints of the optimization problem include periodic data generation, transmission delay and energy requirements. *The scheduling algorithm first of all should guarantee that the sensor node with packet generation period T_i is allocated a time slot with period T_i. Moreover, the length of the allocated time slot should be fixed over all periods and less than the delay requirement. Furthermore, the energy consumed for the transmission of each sensor should be less than its energy requirement.* Let s_i be the ratio of the packet generation period T_i to the subframe length S. We now show that the allocation of a fixed length time slot with period T_i can be achieved by the allocation of fixed length time slot every s_i subframes then arranging the time slots of the nodes within each subframe considering their priorities.

Lemma 1. *Let the optimization problem allocate a time slot of fixed length t_i every s_i subframes to node i where $i \in [1, L]$. If the time slots of the nodes are arranged considering their priorities within each subframe, two consecutive time slots allocated to sensor node i is exactly separated by its packet generation period T_i for all $i \in [1, L]$.*

Proof: Suppose that after the allocation of the time slots of each node i every s_i subframes and arranging them considering the priorities of the sensor nodes within each subframe, two consecutive time slots allocated to sensor i is not separated by its packet generation period T_i. This means that the time slot of sensor i is not in the same relative location within a subframe so there is at least one sensor, say sensor k, with higher priority that is scheduled in one of those subframes and is not scheduled in the other one. However, since those two subframes are separated by s_i and $s_i = m \times s_k$ where m is a positive integer greater than or equal to 1, if sensor k is allocated in one of those subframes, then it must be allocated in the other subframe too. This is a contradiction. □

The periodic data generation requirement of the sensor nodes can there-

fore be restated as *the time slot of fixed length t_i with packet generation period T_i should be allocated to node i every s_i subframes. The time slots of the nodes then need to be arranged considering priorities of the nodes within each subframe to have a separation of T_i between two consecutive time slots allocated to link i.*

We will now formulate and solve this optimization problem for one ECU and multiple ECU cases.

Chapter 4

One ECU Case

4.1 Optimization Problem

The optimal scheduling, rate adaptation and power control problem discussed in Chapter 3 is mathematically formulated for one ECU case where concurrent transmissions are not possible as

minimize

$$\max_{j\in[1,M]} \sum_{i=1}^{L} z_{ij} t_i \tag{4.1}$$

subject to

$$\sum_{j=k}^{k+s_i-1} z_{ij} = 1 \quad \textbf{for} \quad k \in [1, M - s_i + 1], i \in [1, L] \tag{4.2}$$

$$t_i \leq d_i \quad \textbf{for} \quad i \in [1, L] \tag{4.3}$$

$$t_i \left(p_i + p_{tx}\right) \leq e_i \quad \textbf{for} \quad i \in [1, L] \tag{4.4}$$

$$p_i \leq p_{max} \quad \textbf{for} \quad i \in [1, L] \tag{4.5}$$

$$t_i = \frac{L_i}{x_i} \quad \textbf{for} \quad i \in [1, L] \tag{4.6}$$

$$x_i \leq K \frac{p_i h_{ii}}{\beta_i N_0} \quad \textbf{for} \quad i \in [1, L] \tag{4.7}$$

variables

$$x_i \geq 0, \quad p_i \geq 0, \quad z_{ij} \in \{0,1\} \quad i \in [1,L], j \in [1,M] \tag{4.8}$$

where M is the number of subframes in a frame given by the ratio of the frame length F which is equal to the maximum packet generation period T_L, i.e. $F = T_L$, to the subframe length S, i.e. $M = F/S$, t_i is the length of the time slot allocated to the link i, L_i is the packet length of sensor i, p_{tx} is the transmitter circuitry power, p_{max} is the maximum allowed power determined by the UWB regulations, e_i is the maximum allowed energy consumption for sensor i to transmit one packet and z_{ij} is an integer variable taking value '1' if sensor i is allocated to subframe j and value '0' otherwise.

The goal of the optimization problem is to minimize the maximum total active length of all subframes. Equations (4.2), (4.3) and (4.4) represent the periodic packet generation, transmission delay and energy consumption requirements respectively. Equations (4.5), (4.6) and (4.7) on the other hand give the constraint on the maximum power level determined by the UWB regulations, the expression for the time slot length required for the transmission of one packet and the upper bound on the transmission rate given in Equation (2.1) adjusted for the case where there are no concurrent transmissions, i.e. zero interference, respectively.

The variables of the problem are $z_{ij}, i \in [1,L], j \in [1,M]$, representing scheduling, $p_i, i \in [1,L]$, i.e. power allocation, $x_i, i \in [1,L]$, i.e. rate allocation. t_i is not included as an additional variable since there is one-to-one correspondence between t_i and x_i given L_i for each link $i \in [1,L]$.

We now show that the optimal power and rate allocation is independent of the optimal scheduling algorithm, and formulate these two problems separately.

4.2 Optimal Power and Rate Allocation

Due to the assumption of no concurrent transmissions, we consider one link at a time. When the maximum transmission rate in Equation (4.7) is used

given the transmission power, both the time slot length and the energy consumption in Equations (4.6) and (4.4) respectively are minimized. Hence, for an arbitrary transmit power p_i for each link i in the network, the optimal data rate x_i is given by

$$x_i = K\frac{p_i h_{ii}}{\beta_i N_0} \tag{4.9}$$

Increasing the transmit power p_i of the link i increases the maximum achievable rate decreasing the transmission time t_i. Moreover, by combining Equation (4.4) for link energy, Equation (4.6) for transmission time and Equation (4.9) for optimal rate allocation, we obtain the following equation for the energy consumption:

$$E_i = \frac{\beta_i N_0 L_i}{K h_{ii}}(1 + \frac{p_{tx}}{p_i}) \tag{4.10}$$

The energy consumption is also minimized when p_i is assigned to the maximum value. Upper bounded by the regulations as given in Equation (4.5), the optimal transmission power is therefore $p_i = p_{max}$ for each link i. The optimal rate allocation is then

$$x_i = K\frac{p_{max} h_{ii}}{\beta_i N_0} \tag{4.11}$$

for each link i.

4.3 Optimal Scheduling Problem

Since the optimal power and rate allocation minimizes both the time slot length and the energy consumption, the scheduling problem can be separated from the power and rate allocation problem. If the optimal power and rate values do not satisfy the constraints in Equations (4.3) and (4.4) respectively, a feasible schedule cannot be found for the given network. Otherwise, the constraints in Equations (4.3), (4.4), (4.5), (4.6) and (4.7) are satisfied minimizing the time slot length t_i for each link i. The optimal scheduling problem is therefore decomposed from the optimal power and rate allocation problem and can be formulated as a Mixed Integer Linear Programming (MILP) problem as follows:

minimize t

subject to

$$\sum_{j=k}^{k+s_i-1} z_{ij} = 1 \quad \textbf{for} \quad k \in [1, M - s_i + 1], i \in [1, L] \tag{4.12}$$

$$\sum_{i=1}^{L} z_{ij} t_i \leq t \quad \textbf{for} \quad j \in [1, M] \tag{4.13}$$

variables

$$z_{ij} \in \{0, 1\} \quad \textbf{for} \quad j \in [1, M], i \in [1, L], \quad t \geq 0 \tag{4.14}$$

where $t_i = \frac{L_i \beta_i N_0}{K p_{max} h_{ii}}$ for $i \in [1, L]$. Equation (4.12) is the same as Equation (4.2) representing the packet generation period requirement. Equation (4.13) is used to transform the objective from a non-linear form of minimizing $\max_x f(x)$ to a linear form. The variables of the problem are $z_{ij}, i \in [1, L], j \in [1, M]$ and the continuous variable t representing maximum total active length of the subframes.

4.4 NP-Hardness Of The Scheduling Problem

Theorem 1. *The scheduling problem formulated in Chapter 4.3 is NP-Hard.*

Proof: We reduce the NP-hard Minimum Makespan Scheduling Problem (MSP) on identical machines to our scheduling problem. Given a set of n jobs with processing times $pt_i, i \in [1, n]$ and m identical machines, the MSP aims to find an assignment of the jobs to m identical machines such that the makespan, which is the time until all jobs have finished processing, is minimized.

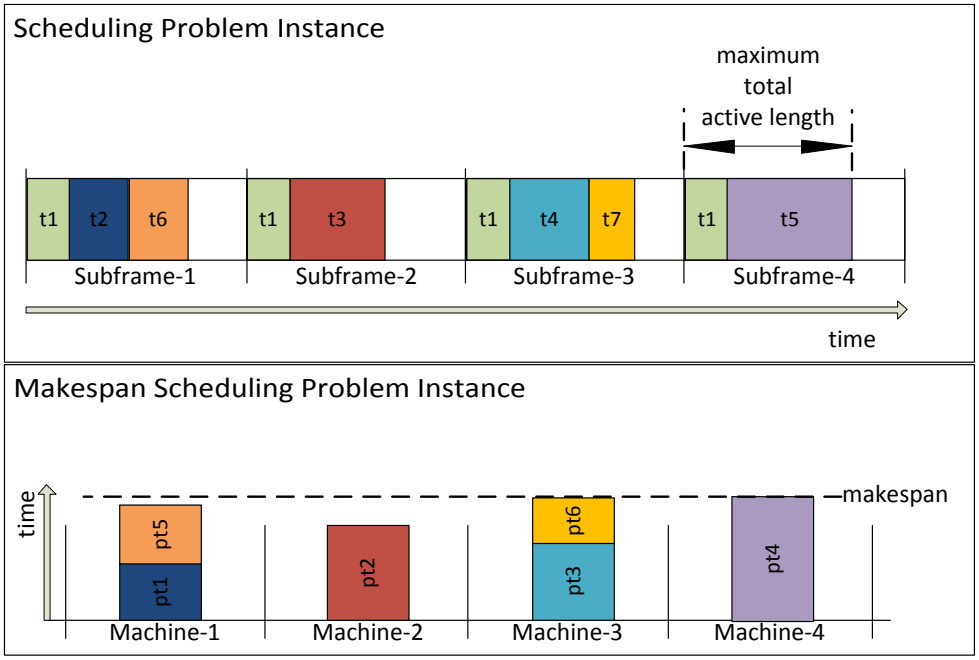

Figure 4.1: MSP Analogy.

Let us define a problem instance where we need to schedule 1 sensor with packet generation period T_1 and time slot length t_1, and n sensors with equal packet generation periods such that $T_2 = T_3 = ... = T_{n+1}$ and time slot length t_i where $i \in [2, n+1]$. Assume that $T_2 = mT_1$ where m is an integer greater than 1. Since the frame length F and the subframe length S are equal to the maximum and minimum of the packet generation periods respectively, the frame of length $F = T_2$ contains m subframes of length $S = T_1$. It is evident that the sensor with packet generation period T_1 is allocated one time slot of length t_1 in each subframe. Let $t_{i+1} = pt_i$ for all $i \in [1, n]$. The problem is then to allocate n sensors of different time slot lengths to m subframes such that the maximum total active length of all the subframes is minimized. We assume that the optimal solution of this instance is less than the subframe length S.

The minimum value of the maximum total active length of all the subframes is equal to t_1 plus the minimum value of the makespan for the MSP defined above. The analogy is illustrated in Fig. 4.1 for the instance where

$m = 4$ and $n = 6$. Since MSP is NP-hard and we can reduce the MSP to an instance of the scheduling problem formulated in Chapter 4.3, the scheduling problem formulated in Chapter 4.3 is also NP-hard. □

Since the problem is NP-hard, we now propose a polynomial time heuristic algorithm.

4.5 Smallest Period into Shortest Subframe First (SSF) Scheduling Algorithm

The analogy between the MSP and the scheduling problem formulated in Chapter 4.3 suggests the use of the polynomial algorithms designed for the MSP for designing a polynomial algorithm for the scheduling problem. List Scheduling [44] algorithm designed for the MSP schedules the jobs in an arbitrary order to the machines with minimum current load at that time. In the following, we propose a scheduling algorithm that similarly assigns the time slots to the subframe with the smallest total active length at that time and illustrate the performance of the algorithm using the analogy between the MSP and the scheduling problem formulated in Chapter 4.3.

Input: Packet generation periods and time slot lengths of L sensors *Output:* Schedule for node transmissions
1: begin **2:** order the nodes in decreasing priority **3:** subframe length $S = T_1$ **4:** frame length $F = T_L$ **5:** number of subframes $M = F/S$ **6:** for $i = 1$ to L **7:** allocate sensor i to the subframe of smallest total **8:** active length **9:** repeat the time slot of sensor i every s_i subframes **10:** end **11:** end

Figure 4.2: SSF Scheduling Algorithm.

SSF Scheduling Algorithm is illustrated in Figure 4.2. The input to the

algorithm are the packet generation periods and the time slot lengths of L sensors. The goal of the algorithm is to assign the time slots of the sensors such that the sensor i is allocated a time slot of length t_i separated by T_i where $i \in [1, L]$.

In the initialization step, the nodes are ordered in decreasing priority. The length of the subframe and frame are S and F respectively. The number of subframes in the frame is then the ratio of the frame length to the subframe length, i.e. $M = F/S$. The schedule then assigns each sensor node i to the subframe with the minimum total active length and then repeats the time slot assignment every s_i subframes for $i \in [1, L]$ in the decreasing priority order. This guarantees that all the time slot allocations are separated by T_i as stated in Lemma 1.

We first illustrate how the SSF Scheduling Algorithm works with an example then derive the properties of the algorithm. Consider an IVWSN consisting of 5 automotive sensors. The packet generation periods of the sensors are $T_1 = T_2 = 1ms$, $T_3 = T_4 = 2ms$ and $T_5 = 4ms$. The corresponding time slot lengths of the sensors are $t_1 = 0.2ms$, $t_2 = 0.1ms$, $t_3 = 0.2ms$, $t_4 = 0.1ms$ and $t_5 = 0.3ms$. For this network, the frame length is $F = 4ms$ consisting of 4 subframes each with length $S = 1ms$ in the initialization step. The scheduling order of the sensor nodes are $1 - 2 - 3 - 4 - 5$ considering their predetermined priorities. The scheduling of the sensor nodes is then illustrated in Figure 4.3(a-e). Each sensor node is first scheduled to the subframe with the smallest total active length and then periodically extended to the entire frame. At the end of the scheduling phase, we have the schedule illustrated in Figure 4.3(e).

We now continue with the properties of the SSF Scheduling Algorithm.

Lemma 2. *The subframes a sensor i is allocated to by SSF Scheduling Algorithm have the same total active lengths just before the scheduling of sensor i. Hence, two consecutive time slots allocated to sensor i is exactly separated by its packet generation period T_i.*

Proof: Suppose that two subframes to which the sensor i with packet generation period T_i is assigned have different total active lengths just prior to the scheduling of that sensor. This means that there is at least one sensor, say sensor k with packet generation period T_k, which is scheduled in one of those subframes and is not scheduled in the other one. However, since those two subframes are separated by s_i subframes and $s_i = m \times s_k$ where m is a positive integer due to the order of scheduling in SSF Scheduling Algorithm, if sensor k is allocated in one of those subframes, then it must be allocated in the other subframe too. This is a contradiction. □

Lemma 3. *Let us define the MSP on identical machines such that there are F/T_i jobs with processing time t_i for each and every $i \in [1, L]$ and F/S identical machines to process these jobs where F and S are the frame and subframe lengths respectively. This is the same as the optimal scheduling problem defined in Chapter 4.3 except that the MSP ignores the requirement of the separation of the time slot allocations to each sensor i by s_i subframes in the scheduling problem defined in Chapter 4.3. Let us denote the makespan of the optimal solution of this MSP and the maximum total active length at the optimal solution of the scheduling problem defined in Chapter 4.3 by OPT_1 and OPT_2 respectively. Then, $OPT_1 \leq OPT_2$.*

Proof: If inequality $OPT_1 \leq OPT_2$ does not hold, OPT_1 is not optimal for MSP since the solution of the scheduling problem is a feasible solution for MSP.□

Theorem 2. *SSF Scheduling Algorithm is a 2-approximation algorithm.*

Proof: First, we will show that the SSF Scheduling Algorithm runs in polynomial time of the input size. Suppose that a schedule with M subframes will be constructed by the allocation of L sensors. The allocation of each sensor require determining the subframe with the smallest total active length,

periodic repetition of the time slot allocation over the entire frame and update of the subframe total active lengths each of which require $O(M)$ unit time. For L sensors, the overall complexity of the allocation is then $O(LM)$ which is polynomial in the input size since $(L+M)^2 \geq LM$.

Now, the proof proceeds as follows. List Scheduling Algorithm proposed for solving the MSP on identical machines [44] assigns jobs to the machines with the minimum current load. The SSF algorithm similarly finds the subframe of minimum total active length for the assignment of each sensor. The periodic extension of the time slot allocation to the other subframes for each sensor is also actually assigning to the subframes of minimum total active length since these subframes all have the same total active length just prior to the scheduling of that particular sensor due to Lemma 2. Since List Scheduling is a 2-approximation algorithm for the MSP [44] and the optimal of the MSP is less than that of our scheduling problem due to Lemma 3, SSF Scheduling Algorithm is a 2-approximation algorithm for the scheduling problem defined in Chapter 4.3.□

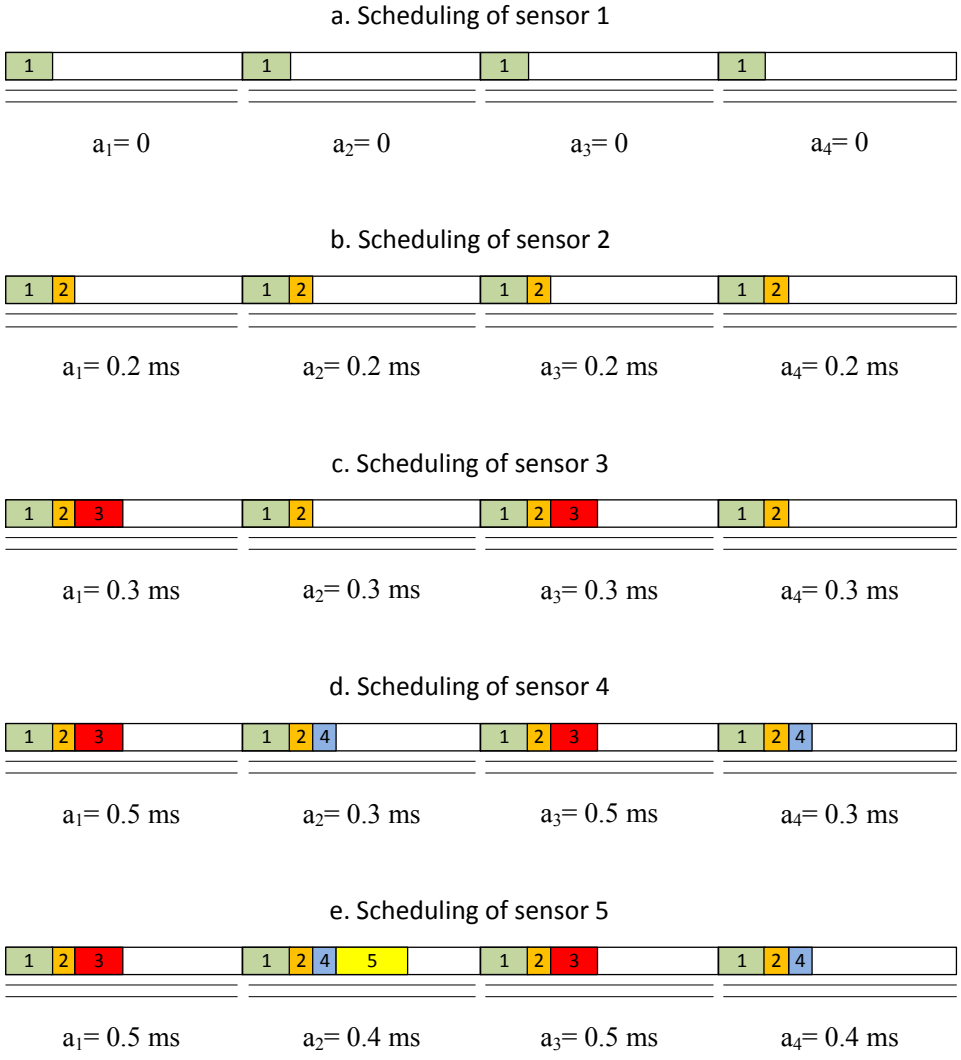

Figure 4.3: The scheduling of the sensor nodes in SSF scheduling algorithm for an IVWSN consisting of 5 automotive sensors with packet generation periods $T_1 = T_2 = 1ms$, $T_3 = T_4 = 2ms$, $T_5 = 4ms$ and corresponding time slot lengths $t_1 = 0.2ms$, $t_2 = 0.1ms$, $t_3 = 0.2ms$, $t_4 = 0.1ms$ and $t_5 = 0.3ms$. Figures (a-e) illustrates the scheduling of each sensor node based on the total active lengths of the subframes. The values of the total active lengths of the subframes shown for the scheduling of each sensor are the values just before the scheduling of that particular sensor.

Chapter 5

Multiple ECU Case

In the previous chapter, we focused on determining optimal scheduling, rate adaptation and power control problem based on the assumption that the IVWSN contains one ECU as the common access point of all automotive sensors hence there are no concurrent transmissions. Having multiple ECUs in IVWSN has two advantages. First, the maximum total active length of the subframes decreases even when no concurrent transmissions are allowed. The power loss from each sensor node to the nearest ECU is expected to decrease compared to one ECU case since the distance between them decreases. This increases the rate of each sensor based on Equation (4.9) and decreases the length of the allocated time slot based on Equation (4.6). Second, the maximum total active length of the subframes may further decrease if concurrent transmissions of the links destined to different ECUs are allowed at the cost of increasing their energy consumption compared to the case where no concurrent transmissions are allowed.

As stated in Chapter 2, in the case of multiple ECUs, one of them is selected as the central controller and responsible for the synchronization of the nodes in the network and resource allocation of the active links. In the case where no concurrent transmissions are allowed in multiple ECU case, the central controller schedules the transmissions in a similar way to the one ECU case: First, power and rate allocation of each link is determined using the updated attenuation values h_{ll} for each link l as given in Chapter 4.2

then the scheduling algorithm assigns the time slots to the subframes using the SSF Algorithm given in Chapter 4.5. We therefore focus on exploiting concurrent transmissions for multiple ECUs next.

5.1 Optimal Solution

5.1.1 Optimal Rate Adaptation

Since both the total time spent and the energy consumed in the transmission of a packet decreases at the maximum rate allocation, for an arbitrary set of transmit powers assigned to the links scheduled for concurrent transmissions, the data rate of the link l is given by

$$x_l = K \frac{p_l h_{ll}}{\beta_l \left(N_0 + \sum_{k \neq l} p_k h_{kl} t^{(p)} \gamma \right)} \tag{5.1}$$

for $l \in [1, L]$ based on Equation (2.1). The only difference between Equation (5.1) and Equation (4.9) developed for one ECU case is the extra interference term added to the noise term due to the concurrent transmissions.

5.1.2 Optimal Power Allocation

Since the rate of a link depends on the power allocations of all concurrently active links, the power allocation of a link in the existence of concurrent transmissions cannot be determined considering only that link as we did for the one ECU case. Increasing the transmit power of a link increases the rate of that link but also creates more interference to the transmission of the concurrently transmitting links decreasing their rates.

The previous work on the scheduling of UWB networks is based on the assumption that power control is not needed for concurrent transmissions [14, 21, 22, 23]: Each link in every time slot is allocated either zero power or maximum allowed power. This result however is derived for the goal of maximizing throughput while providing fairness to the nodes, which is solved by maximizing the total transmission rate in each time slot [14]. Even when the minimum per-flow throughput constraints are included [45], these scheduling

algorithms are based on the assumption that the data transmission of each node can be divided into several possibly non-consecutive time slots with different rate assignments due to the concurrent transmission with different set of nodes. In the formulation of optimal power control, we however assume *packetized transmission meaning that the packet transmission cannot be divided into multiple time slots and the rate of packet transmission is constant* since synchronizing the nodes for rate adaptation within a packet transmission require very accurate synchronization on the order of nanoseconds for UWB communications. We next show that power control is needed for packetized transmission.

Theorem 3. *Power control is needed for the concurrent packetized transmissions.*

Proof: Suppose that we have n concurrently transmitting sensors each allocated to the maximum power level p_{max}. With p_{max} power allocation, suppose that each sensor l needs a time duration t_l to send its data packet and consumes an energy of E_l where $l \in [1, n]$. The time slot length required for the concurrent transmission of these n sensors is $\max_{l\in[1,n]} t_l$. Suppose further that for each $l \in [1, n]$, $t_l \leq d_l$ and $E_l \leq e_l$.

Suppose now that $t_k = \max_{l\in[1,n]} t_l$ and $t_j < t_k$ for $j \neq k$ and $j, k \in [1, n]$. Then, if we decrease the transmission power of sensor j slightly by an arbitrarily small amount such that t_j is still less than t_k and delay and energy requirements of sensor j are still satisfied, the transmission time of the sensors except j will decrease due to the decreasing amount of interference created by sensor j. As a result $\max_{l\in[1,n]} t_l$ will decrease. Hence, p_{max} power allocation is not optimal.□

The optimal power allocation for the concurrent transmission of n links is now formulated as a Geometric Programming (GP) problem:

minimize

$$t \tag{5.2}$$

subject to

$$t_l \leq t \quad \textbf{for} \quad l \in [1, n] \tag{5.3}$$

$$t_l \leq d_l \quad \textbf{for} \quad l \in [1, n] \tag{5.4}$$

$$t_l \left(p_l + p_{tx}\right) \leq e_l \quad \textbf{for} \quad l \in [1, n] \tag{5.5}$$

$$p_l \leq p_{max} \quad \textbf{for} \quad l \in [1, n] \tag{5.6}$$

$$t_l = p_l^{-1} \frac{\beta_l L_l N_0}{K h_{ll}} + \sum_{k \neq l} p_k p_l^{-1} \frac{\beta_l L_l h_{kl} t^{(p)} \gamma}{K h_{ll}} \quad \textbf{for} \quad l \in [1, n] \tag{5.7}$$

variables

$$p_l \geq 0 \quad \textbf{for} \quad l \in [1, n], \quad t \geq 0 \tag{5.8}$$

The goal of the problem is to minimize the length of the time slot required for the concurrent transmissions of the sensors given their delay and energy requirements. The length of the time slot required for the concurrent transmission of n links is equal to the maximum of the time slot lengths of these links and denoted by the continuous variable t in the GP formulation. Equation (5.3) is used to transform the objective from a non-linear form of minimizing $\max_{l \in [1,n]} t_l$ to a linear form. Other variables of the problem are p_l, i.e. transmit powers, for $l \in [1, n]$. We do not state t_l as a variable since it can be removed in the formulation by using Equation (5.7). Equations (5.4) and (5.5) represent the delay and the energy requirements of the sensors respectively. Equation (5.6) represents the upper bound on the transmit power of the sensors. Equation (5.7) formulates the time slot length of each individual sensor as a function of the transmit powers of the sensors based on Equations (4.6) and (5.1).

The terms in the formulation can be arranged easily in the form of the classical GP formulation with positive multiplicative constants. The GP with positive multiplicative constants is a special form of convex optimization and can be solved in polynomial time [46] using the solver GGPLAB [47] developed by Stanford University.

5.1.3 Optimal Scheduling

The optimal rate and power allocation formulated in Chapter 5.1.1 and 5.1.2 respectively assume that the nodes that are concurrently transmitting are known. We now formulate the scheduling problem to determine the nodes that transmit concurrently and assign this concurrently transmitting node set to the subframes.

Suppose L sensor nodes in the network have N distinct packet generation periods $\{T_1, T_2, ..T_N\}$. Let L_n be the set of sensors with packet generation period T_n. Let Q_n denote a $|L_n| \times 2^{|L_n|}$ matrix such that the columns of Q_n represent all possible subsets of the set L_n and the element in the i-th row and j-th column of Q_n takes value 1 if the node i is included in the set j and 0 otherwise. Finally, Q is defined as a $L \times G$ matrix where $G = 2^{|L_1|} + 2^{|L_2|} + ... + 2^{|L_N|}$:

$$Q = \begin{bmatrix} Q_1 & 0 & . & . & . \\ 0 & Q_2 & 0 & . & . \\ 0 & 0 & Q_3 & 0 & . \\ . & . & . & . & . \\ 0 & 0 & 0 & 0 & Q_N \end{bmatrix} \tag{5.9}$$

Such a definition of Q is used to allow the concurrent transmission of only the sensors with the same packet generation period so allocate the time slots of the same length over all subframes the sensors are assigned to.

Let A be a $G \times M$ matrix, where M is the number of subframes in the frame, such that the element in the j-th row and k-th column of A, denoted by A_{jk}, takes value 1 if the set j is included in the subframe k and 0 otherwise. The optimal scheduling is then formulated as a MILP problem:

minimize

$$t \tag{5.10}$$

subject to

$$v^{(i)} Q A u_k^{(k+s_i-1)} = 1 \quad \textbf{for } k \in [1, M - s_i + 1], i \in [1, L] \tag{5.11}$$

$$\sum_{j=1}^{G} A_{jk} t_j \leq t \quad \textbf{for} \quad k \in [1, M] \tag{5.12}$$

variables

$$A_{jk} \in \{0, 1\} \quad \textbf{for} \quad j \in [1, G], k \in [1, M], \quad t \geq 0 \tag{5.13}$$

where $u_i^{(k)}$ is a $M \times 1$ matrix such that the elements i through k take value 1 and the remaining elements are 0, $v^{(i)}$ is a $1 \times L$ matrix such that the i-th element is 1 and other elements are 0, t_j is the length of the time slot assigned to the node set j determined by the optimal GP formulation given in Chapter 5.1.2. Having an infeasible GP problem for a node set j means that the concurrent transmission of this node set is not possible while satisfying the delay and energy requirements of the sensor nodes hence t_j should be set to a large value, say the frame length, to avoid choosing the node set j in the solution of the optimization problem.

The variables of the MILP problem are A_{jk} where $j \in [1, G]$, $k \in [1, M]$ and the continuous variable t representing maximum total active length of the subframes. Equation (5.11) represents the periodic data generation requirement of the sensors. The matrix QA represents the allocation of the sensor nodes to the subframes such that the element of QA in the i-th row and k-th column takes value 1 when node i is allocated to the subframe k and 0 otherwise. When we multiply $v^{(i)}$ with QA, we get the i-th row of the QA matrix which gives the allocation of node i in the subframes. Multiplying $v^{(i)}QA$ by $u_k^{(k+s_i-1)}$ sums s_i consecutive allocations of node i. Equalizing this sum to 1 for each $k \in [1, M - s_i + 1]$ is then used to satisfy the periodic data generation requirement of node i. Equation (5.12) is used to transform the objective from a non-linear form of minimizing maximum total active length of the subframes to a linear form as done in the formulation of one ECU case.

The number of the variables in the MILP problem is exponential in the number of the links resulting in exponential time complexity. The optimal scheduling problem for multiple ECUs is NP-Hard since one ECU is a special case of the multiple ECU problem and is shown to be NP-hard in Chapter 4.4. We will now develop a heuristic algorithm that guarantees to decrease the maximum total active length of the subframes compared to the case

where no concurrent transmissions are allowed while still satisfying the packet generation period, delay and energy requirements of the sensors.

5.2 Maximum Utility based Concurrency Allowance (MUCA) Scheduling Algorithm

MUCA scheduling algorithm is based on improving the performance of the SSF scheduling algorithm proposed for one ECU case through concurrent transmissions. Following the assignment of the nodes to the subframes based on the SSF scheduling algorithm, the set of nodes of maximum utility among the nodes assigned to the subframe of maximum total active length and having the same packet generation period are chosen for concurrent transmissions decreasing the maximum total active length of the subframes in each iteration. The algorithm stops when the value of the maximum total active length cannot be reduced further by concurrent transmissions.

Let us first define the utility function for concurrent transmissions. Suppose that when there are no concurrent transmissions, sensors 1,2,...,n have time slots of lengths t_1,t_2,...,t_n respectively. The total time required for the transmission of these sensors is then $t_1+t_2+...+t_n$. When these n sensors are allocated concurrently with optimal power allocation determined by the GP formulation in Chapter 5.1.2, sensors 1,2,...,n require a time slot of length $t_{\{1,2...,n\}}$. The utility function for the concurrent transmission of the sensors 1,2,...,n is defined as

$$u_{\{1,2...,n\}} = \sum_{i=1}^{n} t_i - t_{\{1,2...,n\}} \tag{5.14}$$

to measure the amount of decrease in the total active length of the subframe by concurrent transmissions. The larger the value of the utility function, the higher the gain from concurrent transmissions. The decision for concurrent transmission is made for positive utility function since a positive utility value corresponds to a decrease in the time duration required for the transmission of the sensors 1,2,...,n.

MUCA algorithm uses utility function to determine the best subset of the nodes in the same subframe with the same packet generation period for concurrent transmissions: The subset that maximizes utility decreases the total active length of the subframe most. Finding the best subset however requires evaluating the utility function for each and every possible subset of nodes. The complexity of this search is exponential. We therefore propose a greedy algorithm that searches for the subset of concurrent transmissions by including the node that maximizes utility one-by-one which we call Concurrency Set Construction (CSC) algorithm.

Input: S: set of nodes considered for concurrent transmissions
Output: G: subset of S that includes all the nodes that are allowed to concurrently transmit

```
1:  begin
2:    G = ∅;D = S;
3:    pick an arbitrary link i ∈ D;
4:    G = G + i;
5:    D = D − i;
6:    while (G ≠ S)
7:      if (max_{i∈D} u_{G+i} > u_G)
8:        k = arg max_{i∈D} u_{G+i};
9:        G = G + k;
10:       D = D − k;
11:     else
12:       break;
13:     end
14:   end
15: end
```

Figure 5.1: Concurrency Set Construction (CSC) algorithm

CSC algorithm shown in Figure 5.1 is described next. S is the set of nodes considered for concurrent transmissions. G is the subset of S that will include all the nodes that are allowed to concurrently transmit at the end of the algorithm: G is initialized to $\emptyset$ (Line 2) and extended to include the node that maximizes utility function when included in G in each iteration (Lines $7-10$). D is the subset of S that includes the nodes considered for concurrent

transmissions in each iteration, i.e. $D = S - G$: In the initialization step, an arbitrary node $i \in D$ is included in the set G (Line 3) whereas in the following iterations, the node $i \in D$ that maximizes the utility when added to G (Line 8) is included in the set G. The condition for stopping the algorithm is either choosing all the nodes in S for concurrent transmissions (Line 6) or not improving the utility by the addition of any of the nodes (Lines 7 and $11 - 13$).

We now describe the MUCA Algorithm illustrated in Figure 5.2. The algorithm starts by the assignment of the nodes to the subframes using the SSF Algorithm (Line 2) then continues by determining the subset of nodes that can reduce the maximum total active length by concurrent transmissions (Lines $3 - 18$). M denotes the number of subframes in the frame, i.e. $M = F/S$, whereas N denotes the number of distinct packet generation periods such that $T_1 < T_2 < ... < T_N$ and $N \leq L$. We define the set of nodes with packet generation period T_j and assigned to the subframe i as S_{ij}. In each iteration of the algorithm, the subframe with the maximum total active length is determined (Line 4) and a subset of the nodes assigned to this subframe with the same packet generation period that are not concurrently transmitting with any other node is chosen for concurrent transmissions using the CSC algorithm described in Figure 5.1 (Lines $7 - 11$). If such a subset is determined for concurrent transmission, i.e. the utility value for the determined subset is positive (Line 12), the schedule in the subframe is updated (Line 13) and repeated with the packet generation period (Line 14). The nodes are scanned for concurrent transmissions starting from the largest packet generation period (Line 6) since these changes affect a smaller number of subframes. If no concurrent transmission can produce a positive utility (Line 18), the algorithm stops.

Input: Packet generation periods, delay and energy requirements of L sensors, attenuation of the links
Output: Schedule for node transmissions

```
1: begin
2:   run SSF Algorithm;
3:   repeat
4:     k=argmax_{j∈[1,M]} a_j ;
5:     u = 0;
6:     for j = N to 1
7:       if S_kj ≠ ∅
8:         apply CSC algorithm to the set S_kj excluding
9:          concurrent transmissions;
10:         u=utility value of the set returned by CSC;
11:      end
12:      if u > 0
13:        update schedule of the k-th subframe;
14:        repeat k-th subframe schedule with period T_j;
15:        break;
16:      end
17:    end
18:  until u = 0
19: end
```

Figure 5.2: Maximum Utility based Concurrency Allowance (MUCA) Scheduling Algorithm.

Chapter 6

Simulations and Performance Evaluation

The goal of this chapter is to evaluate the performance of the proposed SSF and MUCA scheduling algorithms.

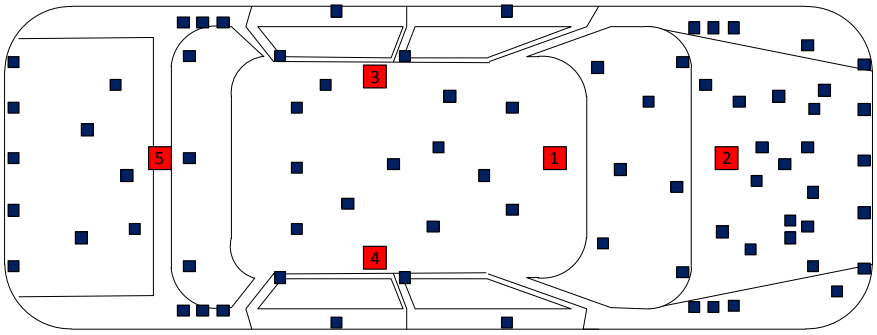

Figure 6.1: A typical 2-D illustration of the IVWSN Topology. Red enumerated boxes represent ECUs and blue boxes represent automotive sensors.

In the simulations, automotive sensors are located considering their approximate real places and their densities in different parts of the vehicle as shown in Figure 6.1 [48]. The results for different number of nodes are averages of the performance of 100 different random selection out of these

predetermined sensor locations. The ECUs are enumerated as shown in Figure 6.1 such that the ECUs are chosen in increasing enumeration, e.g if one ECU is used in a vehicle, the ECU labelled with 1 is used, if two ECUs are used in a vehicle, the ECUs labelled with 1 and 2 are used. Sensor nodes choose the nearest ECU for communication. The packet generation periods of the sensor nodes are uniformly distributed among the nodes from the set $\{1, 5, 10, 50, 100, 1000\}ms$ such that a network consisting of L sensors has $L/6$ sensors with each packet generation period from this set. The packet lengths of the automotive sensors are uniformly distributed in $[10, 20]$-byte range.

The attenuation of the links are determined considering both large scale statistics that arise primarily from the free-space loss and vehicular environment affecting the degree of refraction, diffraction, reflection and absorption, and small scale statistics that occur due to multipath propagation and variations in the environment. The dependence of the path loss on distance summarizing large scale statistics is modeled as

$$PL_{[dB]}^{(ls)}(d) = PL_{[dB]}^{(ls)}(d_0) - 10\alpha \log_{10}\left(\frac{d}{d_0}\right) + Z \tag{6.1}$$

where d is the distance between the transmitter and receiver, d_0 is the reference distance, $PL_{[dB]}^{(ls)}(d_0)$ is the path loss at the reference distance in decibels, $PL_{[dB]}^{(ls)}(d)$ is the path loss at distance d in decibels, α is the path loss exponent and Z is zero mean Gaussian random variable with standard deviation σ_z representing random variations in the model [49, 50]. As to the small-scale fading, it has been shown that the UWB fading amplitude can be well fitted by the lognormal distribution [49, 50]. The path loss considering both large scale and small scale statistics is then given by

$$PL_{[dB]}(d) = PL_{[dB]}^{(ls)}(d) + W \tag{6.2}$$

where W is zero mean Gaussian random variable with standard deviation σ_w. The parameters of the model are summarized in Table 6.1 based on the results of the channel measurement campaign beneath a commercial vehicle chassis in [49, 50] and models used in previous UWB based MAC protocol designs in [14, 22]. The values of the parameters used for the calculation of

the energy consumption derived by using the practical values given in [43, 30] are also given in Table 6.1.

α	4	σ_z	3.30	p_{max}	10mW
σ_w	3.52	$PL(d_0)$	30dB	p_{tx}	30mW
d_0	1m	N_0	10^{-8}W/Hz	K	10^6

Table 6.1: Simulation Parameters

Fig.6.2 shows the maximum total active length of the subframes for different number of nodes and different scheduling algorithms including SSF, EDF, LLF and optimal one. The performance of the SSF scheduling algorithm is very close to the optimal one and outperforms the EDF and LLF scheduling algorithms. The maximum value of the approximation ratio of the SSF algorithm is around 1.10, which is much less than the approximation ratio of 2 proved in Theorem 2, where the approximation ratio is defined as the ratio of the maximum total active length of the scheduling algorithm to that of the optimal solution.

Fig. 6.3 shows the approximation ratio of the SSF scheduling algorithm for different path loss exponents and different number of ECUs in a network of 102 nodes without considering concurrent transmissions. The maximum value of the approximation ratio of the SSF scheduling algorithm is 1.12. The effect of the number of ECUs on the approximation ratio is negligible. On the other hand, the approximation ratio slightly increases as the path loss exponent increases for any number of ECUs due to the increase in the variance of the link attenuation so time slot length of the nodes with increasing path loss exponent.

Fig. 6.4 shows the average runtime of the SSF scheduling algorithm and the optimal solution for different number of nodes. The runtime of the SSF algorithm is negligible compared to the runtime of the optimal solution which increases exponentially as the number of nodes increases.

Table 6.2 illustrates the superior adaptivity of the SSF scheduling algorithm over the EDF scheduling algorithm using a metric called *average number of missed deadlines per unit time*, which is defined as the average number of packets that cannot be transmitted successfully within their delay

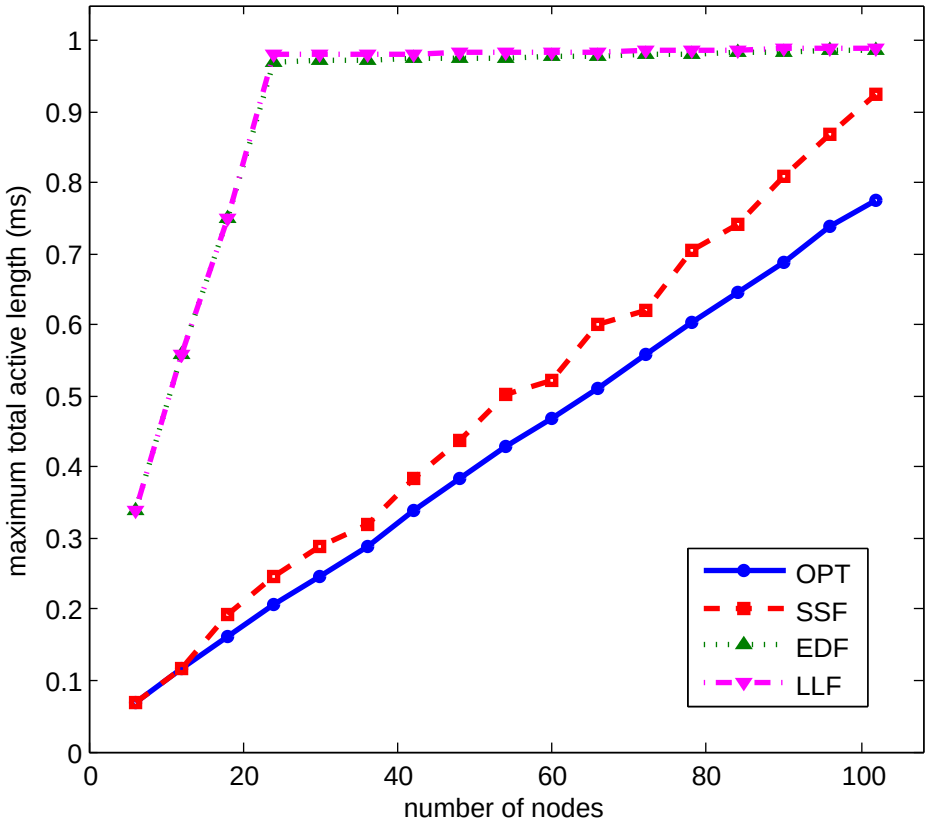

Figure 6.2: Comparison of the maximum total active length of the subframes of the SSF algorithm with EDF, LLF and optimal scheduling algorithms for different number of nodes.

constraint even after considering retransmissions of lost packets in the unallocated parts of the schedule. The SSF scheduling algorithm considerably outperforms the EDF scheduling algorithm in all scenarios. The average number of missed deadlines is greater than 0 for the EDF scheduling algorithm even when the packet loss probability is very small at 10^{-4} due to the non-uniform distribution of the allocations of the packet transmissions over time. Missed deadlines occur in the SSF scheduling only when the packet loss probability is very large at 10^{-1} and number of nodes is 102 where almost 90% of the schedule is allocated.

Fig. 6.5 illustrates the superior adaptivity of the SSF scheduling al-

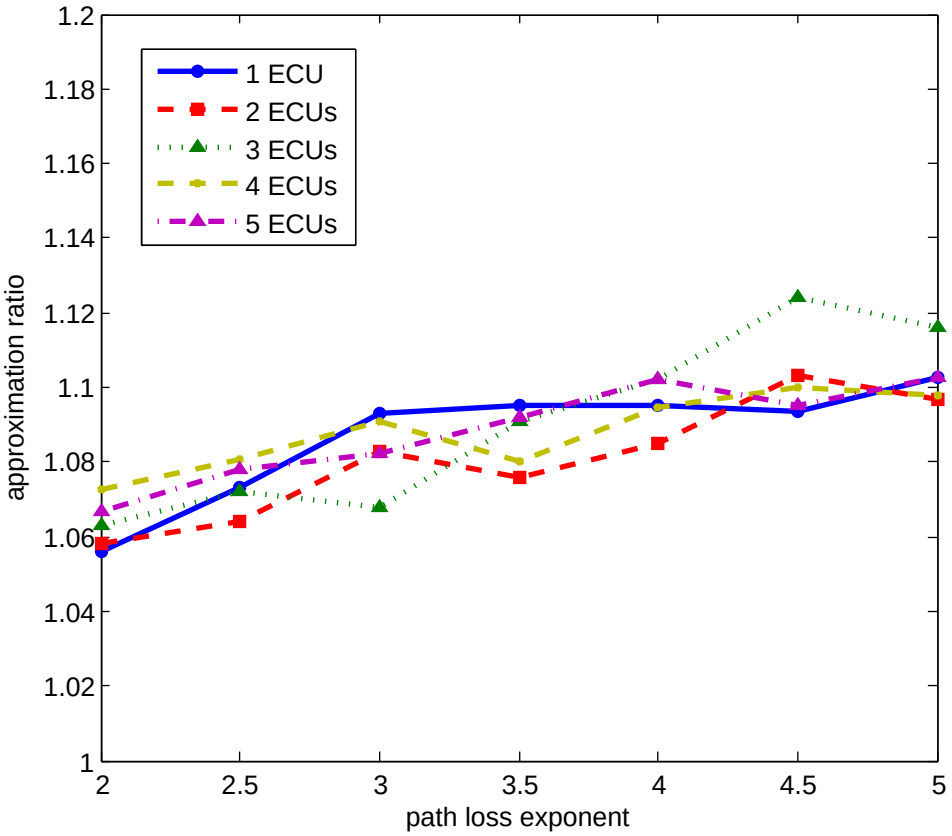

Figure 6.3: Approximation ratio of the SSF scheduling algorithm for different path loss exponents and different number of ECUs in a network of 102 nodes without considering concurrent transmissions.

gorithm over the EDF and LLF scheduling algorithms using another metric called *maximum delay experienced by an aperiodic packet*, which is defined as the worst case delay an aperiodic packet will experience from the packet generation until the transmission in the unallocated part of the schedule. SSF outperforms EDF and LLF algorithms with performance very close to optimal. Since EDF and LLF scheduling algorithms schedules the available data packets as they arrive, some of the subframes are almost fully allocated without leaving any space for the allocation of additional packets. As the number of nodes increases, the number of such fully allocated subframes increases causing the aperiodic packets to wait for multiple subframes until

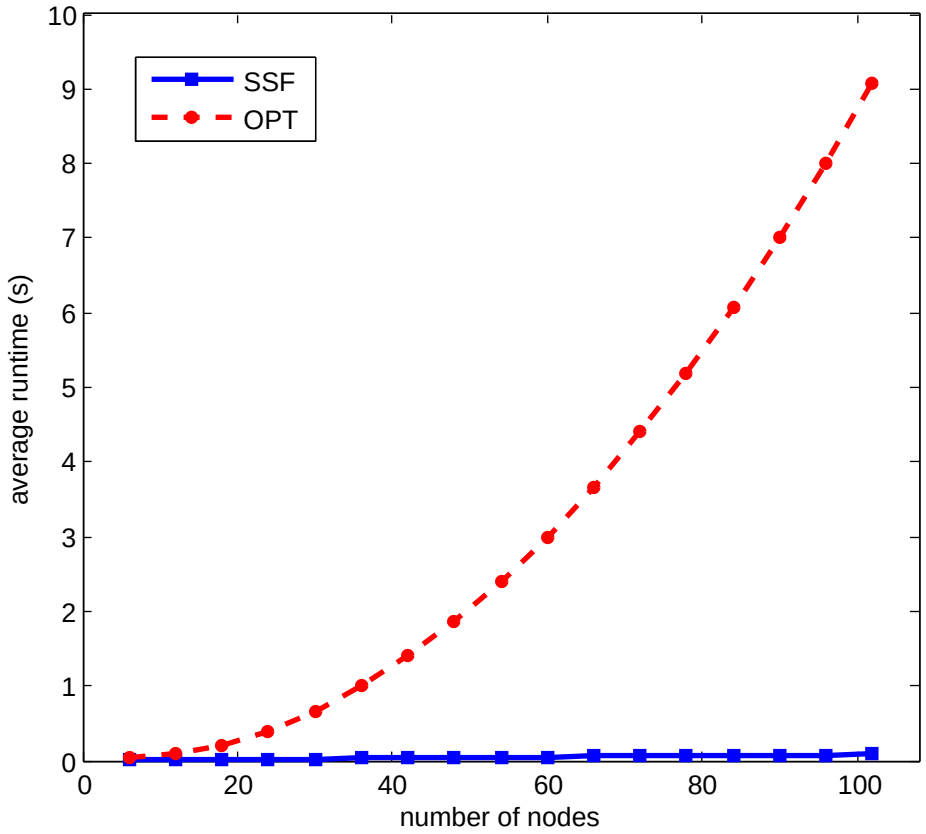

Figure 6.4: Comparison of the average runtime of the SSF and optimal algorithms.

an unallocated part of the schedule. On the other hand, since SSF schedule allocates the data packets as uniformly as possible among the subframes, it can allocate the data packets of the additional messaging in the subframe that they are generated.

Fig. 6.6 shows the maximum total active length of the subframes of the MUCA scheduling algorithm and optimal solution for different number of nodes and different number of ECUs. The approximation ratio of the MUCA algorithm is around 1.35 and the performance of the algorithm is robust to the large number of nodes and ECUs.

Fig. 6.7 shows the average runtime of the MUCA scheduling algorithm and the optimal solution for different number of nodes. The average runtime

PLP	OPT 54	SSF 54	EDF 54	OPT 102	SSF 102	EDF 102
10^{-4}	0	0	1.2	0	0	5.5
10^{-3}	0	0	3.1	0	0	38.7
10^{-2}	0	0	11.8	0	0	263.1
10^{-1}	0	0	97.2	0	100.9	2457.8

Table 6.2: Comparison of the average number of missed deadlines per second of SSF, EDF and optimal scheduling algorithms for different number of nodes. PLP denotes packet loss probability.

of the MUCA algorithm is negligible compared to the optimal MILP formulation which increases exponentially as the number of nodes increases. Moreover, increase in the number of ECUs results in a dramatic increase in the runtime of the MILP formulation. On the other hand, the runtime of the MUCA algorithm increases linearly with the number of nodes and is robust to the large number of ECUs.

Fig. 6.8 shows the approximation ratio of the MUCA scheduling algorithm for different path loss exponents and different number of ECUs in a network of 150 nodes. The maximum value of the approximation ratio of the MUCA scheduling algorithm is around 1.4. In contrast to the SSF scheduling algorithm, the number of ECUs increases the approximation ratio of the MUCA algorithm due to the increasing number of the combinations of the links for concurrent transmissions. On the other hand, the approximation ratio of the MUCA algorithm slightly increases as the path loss exponent increases for any number of ECUs similar to the SSF scheduling algorithm.

Fig. 6.9 shows the maximum total active length of the MUCA scheduling algorithm for different delay requirement factors and different number of nodes. Delay requirement factor is defined as the ratio of the delay requirement d_i to the time slot length t_i when there are no concurrent transmissions, denoted by $t_i^{(nc)}$, for each sensor node i in the network. The delay requirement factor is assumed to be the same for each sensor in the network. Since factor 1 corresponds to the case where $t_i^{(nc)} = d_i$ for each node i in the network, concurrent transmission is not allowed: Any concurrent transmission increases the time slot length allocated to the node violating the delay requirement

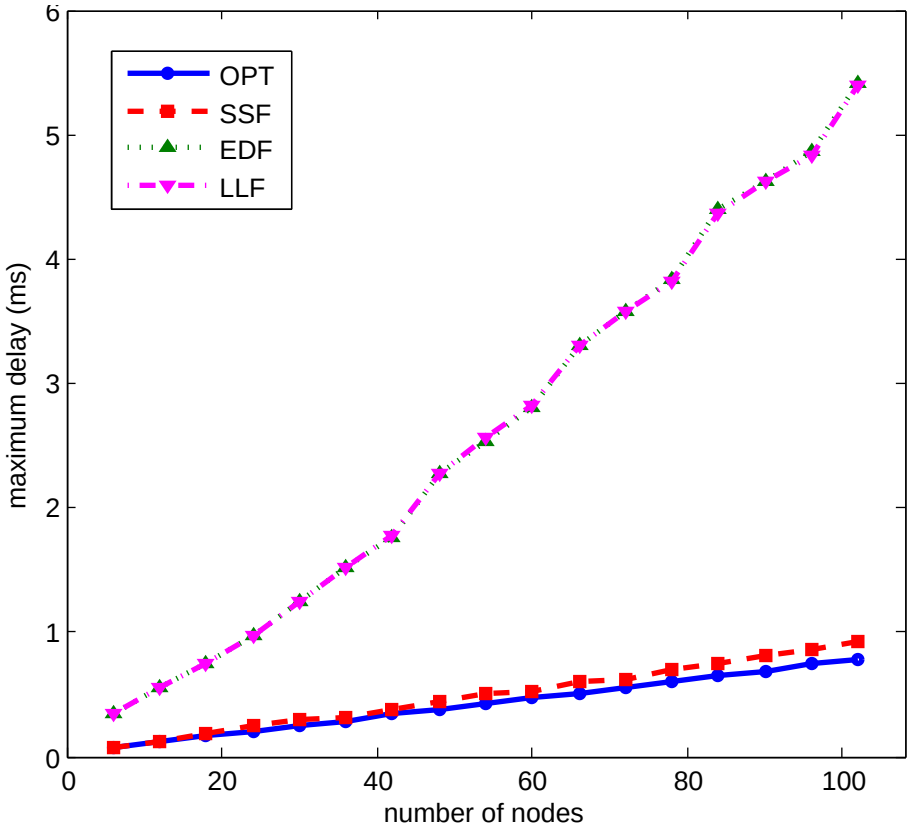

Figure 6.5: Comparison of the maximum delay experienced by an aperiodic packet for SSF, EDF, LLF and optimal scheduling algorithms.

of the sensors. As the delay requirement factor increases, more concurrent transmissions are allowed improving the performance of the MUCA scheduling algorithm. However, the performance gain of the algorithm decreases as the delay requirement factor increases and eventually saturates to 0 for large values of the delay requirement factor: The interference among the concurrent transmissions becomes the limiting factor instead of the delay requirement.

Fig. 6.10 shows the maximum total active length of the MUCA scheduling algorithm for different energy requirement factors and different number of nodes. Energy requirement factor is defined as the ratio of the energy require-

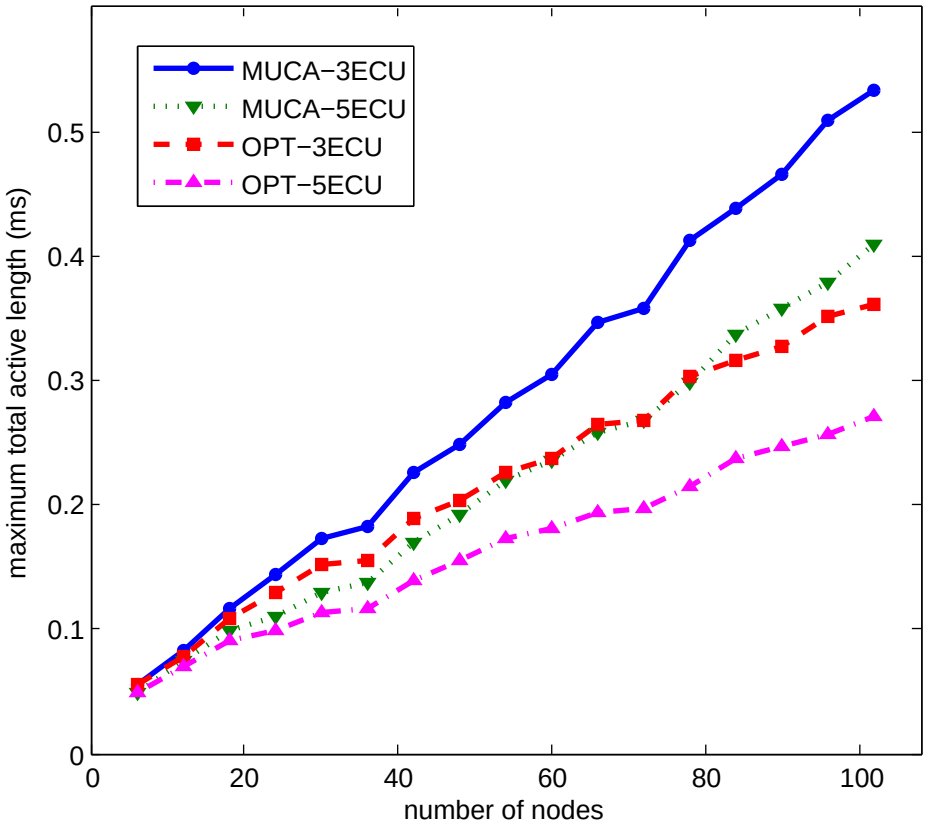

Figure 6.6: Comparison of the maximum total active length of the subframes of the MUCA algorithm with the optimal MILP solution for different number of nodes and ECUs.

ment e_i to the energy consumed during the time slot length t_i when there are no concurrent transmissions, denoted by $E_i^{(nc)}$, for each sensor node i in the network. The energy requirement factor is assumed to be the same for each sensor in the network. The behavior of the curve in Fig. 6.10 is similar to Fig. 6.9: As the energy requirement factor increases, more concurrent transmissions are allowed improving the performance of the MUCA scheduling algorithm. However, the performance gain of the MUCA algorithm saturates faster with the energy requirement factor than the delay requirement factor since the rate of increase in the energy consumption of a sensor node due to concurrent transmissions is slower than that in the time slot length

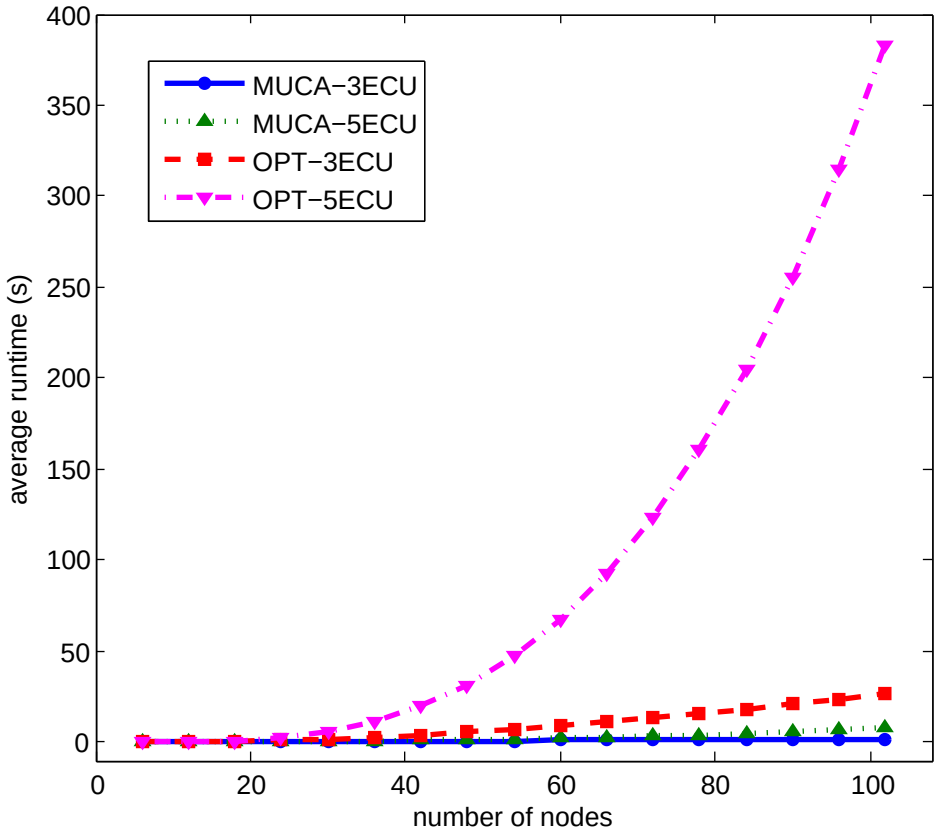

Figure 6.7: Comparison of the average runtime of the MUCA algorithm with the optimal MILP formulation.

allocated to that sensor.

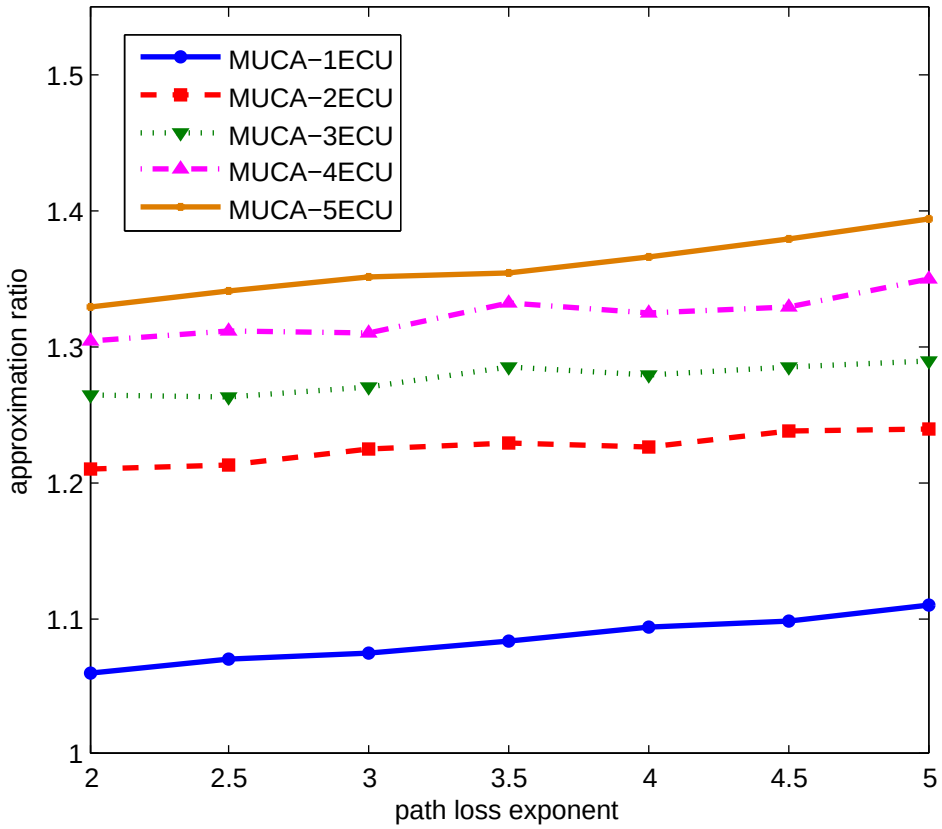

Figure 6.8: Approximation ratio of the MUCA scheduling algorithm for different path loss exponents and different number of ECUs in a network of 150 nodes.

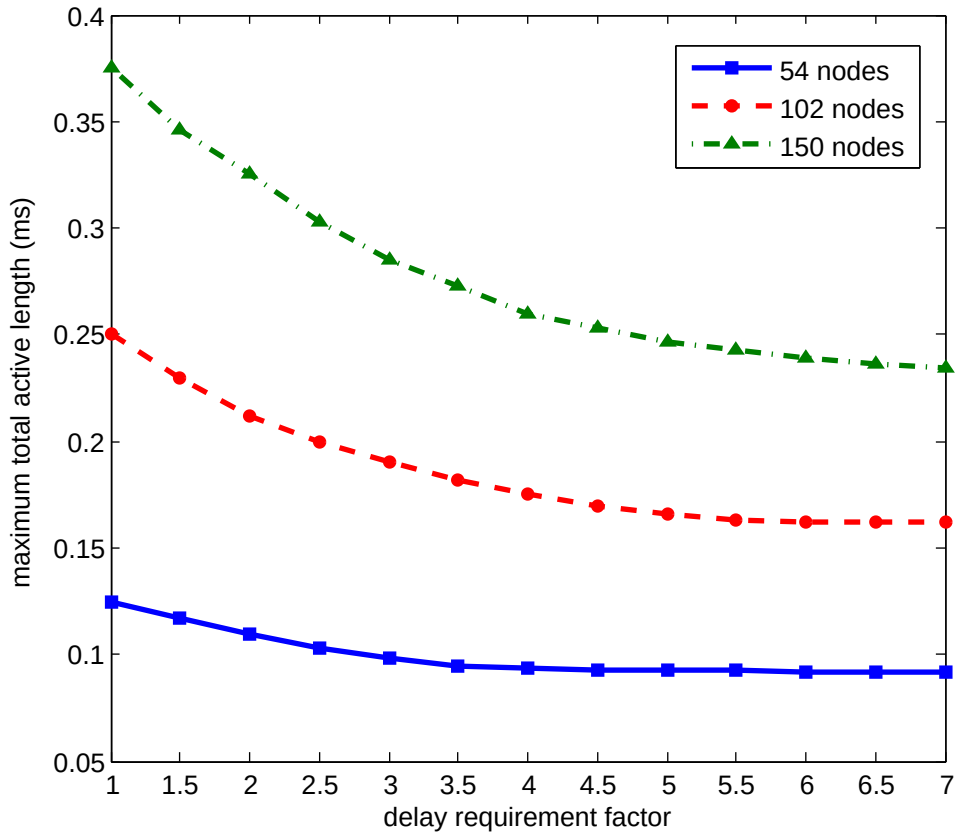

Figure 6.9: Maximum total active length of the MUCA scheduling algorithm for different delay requirement factors and different number of nodes.

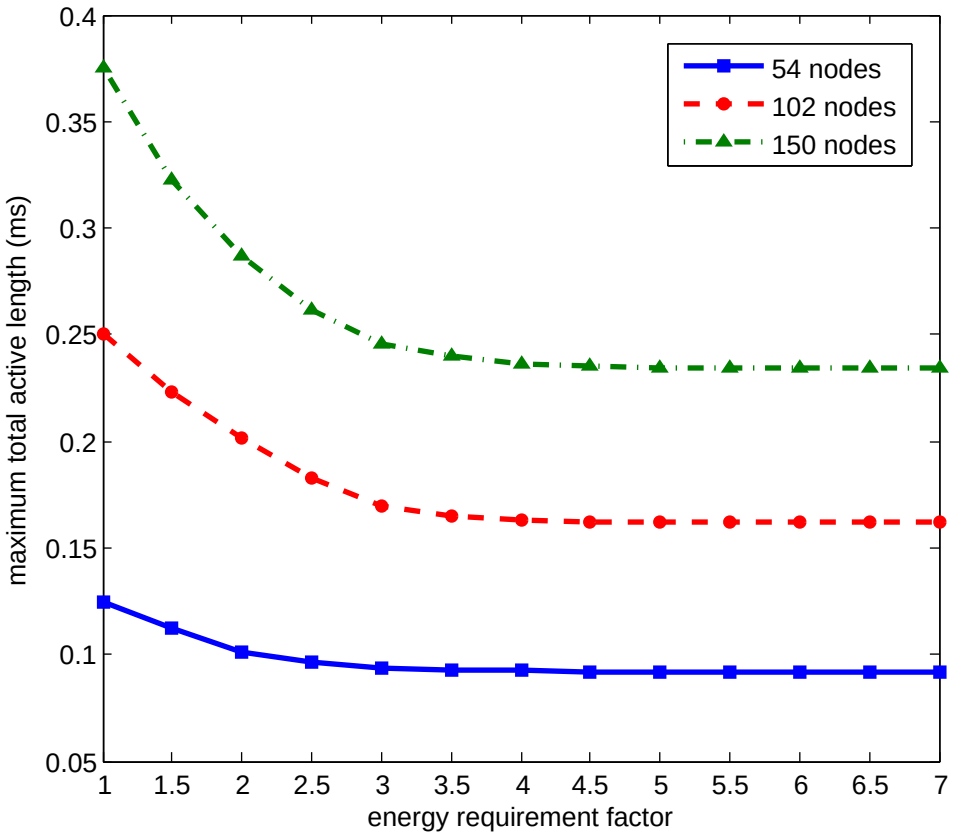

Figure 6.10: Maximum total active length of the MUCA scheduling algorithm for different energy requirement factors and different number of nodes.

Chapter 7

Conclusion

We study optimal power control, rate adaptation and scheduling for UWB-based IVWSNs. A novel scheduling problem has been formulated to provide maximum level of adaptivity accommodating the changes in transmission time, retransmissions due to packet losses and allocation of additional messages while meeting the packet generation period, transmission delay, reliability and energy requirements of the sensor nodes varying over a wide range. Providing maximum level of adaptivity is quantified as minimizing the maximum total active length of all the subframes in a frame, where the subframe and frame are defined as the minimum and maximum packet generation period of the sensor nodes respectively.

For one ECU case where no concurrent transmissions are allowed, the optimal rate and power allocation has been proved to be independent of the optimal scheduling algorithm: Maximum power and rate allocation, i.e. no power control, has been proved to be optimal. The NP-hardness of the scheduling problem has been shown and the optimal solution is formulated as a Mixed Integer Linear Programming (MILP) problem. A 2-approximation algorithm called Smallest Period into Shortest Subframe First (SSF) scheduling algorithm is then proposed as a solution to this scheduling problem. The SSF algorithm has been shown to outperform commonly used Earliest Deadline First (EDF) and Least Laxity First (LLF) scheduling algorithms with approximation ratio less than 1.12 through simulations. Moreover, the su-

perior adaptivity of the SSF over EDF and LLF scheduling algorithms is illustrated by demonstrating its better tolerance to packet failures and smaller worst case delay for additional aperiodic packets.

For multiple ECU case where concurrent transmissions are allowed, it has been proved that power control is needed in contrast to most UWB system formulations: Optimal power control is formulated as a Geometric Programming (GP) problem which is proved to be solvable in polynomial-time. Using the optimal power control, the optimal scheduling problem is then formulated as a MILP problem where the number of variables is exponential in the number of the links. A heuristic algorithm called Maximum Utility based Concurrency Allowance (MUCA) scheduling algorithm is then proposed to improve the performance of the SSF scheduling algorithm iteratively by determining the set of maximum utility at each iteration where the utility of a set is defined as the amount of decrease in the maximum total active length by the concurrent transmissions of the nodes in this set. The algorithm stops when the value of the maximum total active length cannot be reduced further by concurrent transmissions. The MUCA algorithm has been shown to perform very close to optimal with approximation ratio below 1.4.

Using the UWB as the underlying physical layer makes the problems more tractable due to the linear dependency of the transmission rate on SINR. Generalizing the problem and findings for any rate adaptive physical layer will be investigated as part of the future work.

References

[1] N. Navet, Y. Song, F. Simonot-Lion, and C. Wilwert, "Trends in automotive communication systems," *Proceedings of the IEEE*, vol. 93, no. 6, pp. 1204–1223, June 2005.

[2] S. C.Ergen, A. Sangiovanni-Vincentelli, X. Sun, R. Tebano, S. Alalusi, G. Audisio, and M. Sabatini, "The tire as an intelligent sensor," *IEEE Transactions on Computer-Aided Design of Integrated Circuits and Systems*, vol. 28, no. 7, pp. 941–955, July 2009.

[3] M. Ahmed, C.U.Saraydar, T. Elbatt, J. Yin, T. Talty, and M. Ames, "Intra-vehicular wireless networks," in *IEEE Globecom*, November 2007, pp. 1–9.

[4] A. Sangiovanni-Vincentelli and M. D. Natale, "Embedded system design for automotive applications," *IEEE Computer*, vol. 40, no. 10, pp. 42–51, October 2007.

[5] Y. Wu, G. Buttazzo, E. Bini, and A. Cervin, "Parameter selection for real-time controllers in resource-constrained systems," *IEEE Transactions on Industrial Informatics*, vol. 6, no. 4, pp. 610–620, November 2010.

[6] W. Zhang, M. S. Branicky, and S. M. Phillips, "Stability of networked control systems," *IEEE Control Systems*, vol. 21, no. 1, pp. 84–99, February 2001.

[7] J. P. Hespanha, P. Naghshtabrizi, and Y. Xu, "A survey of recent results in networked control systems," *Proceedings of the IEEE*, vol. 95, no. 1, pp. 138–162, January 2007.

[8] W. P. M. H. Heemels, A. R. Teel, N. van de Wouw, and D. Nesic, "Networked control systems with communication constraints: Tradeoffs

between transmission intervals, delays and performance," *IEEE Transactions on Automatic Control*, vol. 55, no. 8, pp. 1781–1796, August 2010.

[9] J. R. Moyne and D. M. Tilbury, "The emergence of industrial control networks for manufacturing control, diagnostics, and safety data," *Proceedings of the IEEE*, vol. 95, no. 1, pp. 29–47, January 2007.

[10] L. Schenato, B. Sinopoli, M. Franceschetti, K. Poolla, and S. S. Sastry, "Foundations of control and estimation over lossy networks," *Proceedings of the IEEE*, vol. 95, no. 1, pp. 163–187, January 2007.

[11] S. C. Smith and P. Seiler, "Estimation with lossy measurements: Jump estimators for jump systems," *IEEE Transactions on Automatic Control*, vol. 48, no. 12, pp. 2163–2171, December 2003.

[12] P. Park, J. Araujo, and K. H. Johansson, "Wireless networked control system co-design," in *International Conference on Networking, Sensing and Control*, April 2011.

[13] A. Balluchi, L. Benvenuti, and A. L. Sangiovanni-Vincentelli, "Hybrid systems in automotive electronics design," *International Journal of Control*, vol. 79, no. 5, pp. 375–405, 2006.

[14] B. Radunovic and J. L. Boudec, "Optimal power control, scheduling, and routing in uwb networks," *IEEE Journal on Selected Areas in Communications*, vol. 22, no. 7, pp. 1252–1270, September 2004.

[15] O. Tonguz, H. Tsai, C. Saraydar, T. Talty, and A. Macdonald, "Intra-car wireless sensor networks using rfid: Opportunities and challenges," in *IEEE Mobile Networking for Vehicular Environments*, May 2007, pp. 43–48.

[16] H. Tsai, W. Viriyasitavat, O. Tonguz, , C. Saraydar, T. Talty, and A. Macdonald, "Feasibility of in-car wireless sensor networks: A statistical evaluation," in *IEEE Sensor, Mesh and Ad Hoc Communications and Networks (SECON)*, June 2007, pp. 101–111.

[17] A. Moghimi, H. Tsai, C. Saraydar, and O. Tonguz, "Characterizing intra-car wireless channels," *IEEE Transactions on Vehicular Technology*, vol. 58, no. 9, pp. 5299–5305, November 2009.

[18] H. Tsai, O. Tonguz, C. Saraydar, T. Talty, M. Ames, and A. Macdonald, "Zigbee-based intra-car wireless sensor networks: A case study," *IEEE Wireless Communications*, vol. 14, no. 6, pp. 67–77, December 2007.

[19] W. Niu, J. Li, and T. Talty, "Intra-vehicle uwb channel measurements and statistical analysis," in *IEEE Globecom*, December 2008, pp. 1–5.

[20] ——, "Ultra-wideband channel modeling for intravehicle environment," *EURASIP Journal on Wireless Communications and Networking - Special number on wireless access in vehicular environments*, pp. 1–12, January 2009.

[21] K. H. Liu, L. Cai, and X. Shen, "Exclusive-region based scheduling algorithms for uwb wpan," *IEEE Transactions on Wireless Communications*, vol. 7, no. 3, pp. 933–942, March 2008.

[22] H. Jiang and W. Zhuang, "Effective packet scheduling with fairness adaptation in ultra-wideband wireless networks," *IEEE Transactions on Wireless Communications*, vol. 6, no. 2, pp. 680–690, February 2007.

[23] K. H. Liu, L. Cai, and X. Shen, "Multiclass utility-based scheduling for uwb networks," *IEEE Transactions on Vehicular Technology*, vol. 57, no. 2, pp. 1176–1187, March 2008.

[24] R. Madan, S. Cui, S. Lall, and A. J. Goldsmith, "Cross-layer design for lifetime maximization in interference-limited wireless sensor networks," *IEEE Transactions on Wireless Communications*, vol. 5, no. 11, pp. 3142–3152, November 2006.

[25] M. Z.Win and R. A. Scholtz, "Ultra-wide bandwidth time-hopping spread-spectrum impulse radio for wireless multiple-access communication," *IEEE Transactions on Communications*, vol. 48, no. 4, pp. 679–689, April 2000.

[26] E. Uysal-Biyikoglu, B. Prabhakar, and A. E. Gamal, "Energy-efficient packet transmission over a wireless link," *IEEE/ACM Transactions on Networking*, vol. 10, no. 4, pp. 487–499, August 2002.

[27] F. Zhang and S. Chanson, "Improving communication energy efficiency in wireless networks powered by renewable energy sources," *IEEE Transactions on Vehicular Technology*, vol. 54, no. 6, pp. 2125–2136, November 2005.

[28] W. Chen and U. Mitra, "Energy efficient scheduling with individual packet delay constraints," in *IEEE INFOCOM*, June 2006, pp. 1–6.

[29] X. Zhong and C.-Z. Xu, "Energy-efficient wireless packet scheduling with quality of service control," *IEEE Transactions on Mobile Computing*, vol. 6, no. 10, pp. 1158–1170, October 2007.

[30] T. Wang, W. Heinzelman, and A. Seyedi, "Link energy minimization in ir-uwb based wireless sensor networks," *IEEE Transactions on Wireless Communication*, vol. 9, no. 9, pp. 2800–2811, September 2010.

[31] T. Elbatt and A. Ephremides, "Joint scheduling and power control for wireless ad hoc networks," *IEEE Transactions on Wireless Communications*, vol. 3, no. 1, pp. 74–85, January 2004.

[32] L. Fu, S. C. Liew, and J. Huang, "Fast algorithms for joint power control and scheduling in wireless networks," *IEEE Transactions on Wireless Communications*, vol. 9, no. 3, pp. 1186–1197, March 2010.

[33] H. C. Foundation, "Wirelesshart." [Online]. Available: http://www.hartcomm.org

[34] ISA, "Isa-100.11a-2009 wireless systems for industrial automation: Process control and related applications." [Online]. Available: http://www.isa.org

[35] I. 802.15.4e, "Ieee 802.15 wpan task group 4e (tg4e)." [Online]. Available: http://ieee802.org/15/pub/TG4e.html

[36] M. Baldi, R. Giacomelli, and G. Marchetto, "Time-driven access and forwarding for industrial wireless multihop networks," *IEEE Transactions on Industrial Informatics*, vol. 5, no. 2, pp. 99–112, May 2009.

[37] B. Demirel, Z. Zou, P. Soldati, and M. Johansson, "Modular co-design of controllers and transmission schedules in wirelesshart," in *IEEE Conference on Decision and Control and European Control Conference*, December 2011.

[38] A. Saifullah, Y. Xu, C. Lu, and Y. Chen, "Real-time scheduling for wirelesshart networks," in *IEEE Real-Time Systems Symposium (RTSS)*, December 2010.

[39] P. Soldati, H. Zhang, and M. Johansson, "Deadline-constrained transmission scheduling and data evacuation in wirelesshart networks," in *European Control Conference*, August 2009.

[40] H. Zhang, F. Osterlind, P. Soldati, T. Voigt, and M. Johansson, "Rapid convergecast on commodity hardware: Performance limits and optimal policies," in *IEEE Conference on Sensor, Mesh and Ad Hoc Communications and Networks (SECON)*, June 2010.

[41] J. Liu, *Real-Time Systems*. Prentice Hall, 2000.

[42] "Ieee standard for information technology - telecommunications and information exchange between systems - local and metropolitan area networks - specific requirement part 15.4: Wireless medium access control (mac) and physical layer (phy) specifications for low-rate wireless personal area networks (wpans)," *IEEE Std 802.15.4a-2007 (Amendment to IEEE Std 802.15.4-2006)*, pp. 1–203.

[43] N. Riaz and M. Ghavami, "An energy-efficient adaptive transmission protocol for ultrawideband wireless sensor networks," *IEEE Transactions on Vehicular Technology*, vol. 58, no. 7, pp. 3647–3660, September 2009.

[44] R. Graham, "Bounds for certain multiprocessing anomalies," *The Bell System Technical Journal*, vol. 45, no. 9, pp. 1563–1581, November 1966.

[45] Z. Yang, L. Cai, and W. S. Lu, "Practical scheduling algorithms for concurrent transmissions in rate-adaptive wireless networks," in *IEEE INFOCOM*, March 2010, pp. 1–9.

[46] S. Boyd and L. Vandenberghe, *Convex Optimization*. Cambridge University Press, 2004.

[47] http://www.stanford.edu/ boyd/ggplab/.

[48] B. GmbH, *Automotive Handbook*. Robert Bosch GmbH, 2007.

[49] C. U. Bas and S. C. Ergen, "Ultra-wideband channel model for intra-vehicular wireless sensor networks," in *IEEE Wireless Communications and Networking Conference (WCNC)*, April 2012.

[50] ——, "Ultra-wideband channel model for intra-vehicular wireless sensor networks beneath the chassis: From statistical model to simulations," *to appear in IEEE Transactions on Vehicular Technology*.